

---

MSc Thesis

---

**Study on the Mechanism of Spontaneous  
Combustion of Coal and Its Index Gases in  
Tingnan Coal Mine**

---

**Author: Yuyi Xie**

**Supervisor: Professor Hongqing Zhu**

Date(04/05/2022)



---

School of Emergency Management and Safety Engineering  
China University of Mining and Technology (Beijing)

Beijing Haidian district Xueyuan Rd,Ding 11.  
Zonghe Building 225





---

## **Declaration of Authorship**

---

„I declare in lieu of oath that this thesis is entirely my own work except where otherwise indicated. The presence of quoted or paraphrased material has been clearly signaled and all sources have been referred. The thesis has not been submitted for a degree at any other institution and has not been published yet.”

---

## Abstract

---

Tingnan Coal Mine is an important coal mine in Shanxi Province, China. The shortest period of spontaneous combustion of the coal seam in Tingnan Coal Mine is 35 days, which determines that the spontaneous combustion tendency of the coal seam is grade one. At the same time, high gas also brought more pressure to Tingnan's fire prevention and daily production work. In this paper, the characteristic temperature point and reaction kinetic parameters of Tingnan coal were analyzed by thermogravimetric experiment, the internal functional group structure of coal was analyzed by FTIR test, and the physical and chemical properties of Tingnan coal were analyzed, thus it was determined that it was flammable. And by using the experimental methods of temperature-programmed oxidation and constant temperature oxidation, the release law of the index gases  $H_2$ ,  $CO$ ,  $CO_2$  and  $C_2H_4$  in the process of coal spontaneous combustion is studied, and the various gases produced in the process of coal spontaneous combustion and their relationship with the change of coal seam temperature are analyzed. , and selected the appropriate proportion of carbon oxides as the index gas for coal spontaneous combustion early warning. This research will help to improve the scientificity and effectiveness of coal mine safety management, and help to ensure the safe production and sustainable development of coal mines.

**Keywords:** coal spontaneous combustion, temperature programmed experiment, index gas, forecasting

---

# Table of Contents

---

Declaration of Authorship .....	I
Abstract .....	II
Table of Contents .....	III
1 Introduction.....	1
1.1 General situation of mine.....	1
1.1.1 Natural conditions.....	1
1.1.2 Mining technological conditions .....	2
1.1.3 Resources reserves .....	3
1.1.4 Minefield development.....	3
1.2 Research status .....	5
1.2.1 Research status of coal spontaneous combustion mechanism .....	5
1.2.2 Research status of coal spontaneous combustion prevention.....	6
1.2.3 Research status of research on prediction and forecast technology of coal spontaneous combustion .....	7
2 Study on the mechanism of coal seam spontaneous combustion .....	9
2.1 Transport and adsorption of oxygen in coal.....	9
2.2 Heating and burning of coal.....	13
3 Experimental Study .....	22
3.1 Introduction to the experimental device .....	22
3.2 Principle of the experiment .....	23
3.2.1 Thermo Gravimetric Analysis (TGA).....	23
3.2.2 Differential Scanning Calorimetry (DSC) .....	24
3.2.3 Fourier Transform Infrared Spectroscopy (FTIR) .....	25
3.3 Influencing factors of the experiment.....	25
3.3.1 Influencing factors of thermogravimetric experiments .....	25
3.3.2 Influencing Factors of Differential Scanning Calorimetry Experiments .....	26
3.3.3 Influence Factors of Fourier Transform Infrared Spectroscopy .....	27
3.3.4 Experiment Procedure.....	27
3.4 Analysis of coal thermo gravimetric analysis .....	28
3.4.1 Influence of oxygen concentration on coal thermo gravimetric experiment .	28
3.4.2 Influence of heating rate on coal thermo gravimetric experiment .....	30
3.4.3 Influence of particle size on coal thermo gravimetric experiment .....	31
3.5 Analysis of coal characteristic temperature points and reaction kinetic parameters .....	33

3.5.1 Calculation of reaction kinetic parameters for coal .....	33
3.5.2 Relationships between characteristic coal temperature points, reaction kinetic parameters and volatiles and elements.....	36
3.5.3 Experimental conclusions.....	40
3.6 Fourier transform infrared spectroscopy of coal .....	41
3.6.1 Characteristic gas analysis for thermal decomposition of coal .....	41
3.6.2 Analysis of the functional groups of coal .....	43
4 Analysis of index gases .....	45
4.1 Analytical study of CO and its indicators .....	45
4.2 Analysis of the effect of wind flow dilution on CO and its indicators .....	47
4.3 Analysis of the effect of nitrogen injection on CO and its indicators .....	51
4.4 Analysis of the effect of gas emergence on CO and its indicators.....	53
4.5 Determination of index gases from natural coal seam fires .....	54
4.5.1 Basis and content of determination .....	54
4.5.2 Principle of determination .....	55
4.5.3 Test equipment.....	56
4.5.4 Experimental steps .....	57
4.5.5 Gas samples Testing.....	58
4.5.6 Measurement results .....	60
5 Conclusion.....	66
Reference.....	68

# 1 Introduction

## 1.1 General situation of mine

### 1.1.1 Natural conditions

Tingnan Minefield is located in the central and western Shaanxi Province, the geographical coordinates are:  $107^{\circ}50'16''$  -  $107^{\circ}57'45''$  east longitude,  $35^{\circ}04'45''$  -  $35^{\circ}07'28''$  north latitude, the area is  $35.5484 \text{ km}^2$ . The topography in the field belongs to the plateau landform, the general trend is high in southwest and low in northeast. The mining area belongs to Jinghe river system. Jinghe River flows from north to south through the eastern part of the mine field, with an average annual flow of  $57.7 \text{ m}^3/\text{s}$ , the minimum flow of  $1.0 \text{ m}^3/\text{s}$  in dry season and the maximum flow of  $8150 \text{ m}^3/\text{s}$  in flood season. The minefield is located in the middle latitude highland area, which belongs to the warm temperate semiarid continental climate. Non-destructive seismic records in the field.



Fig 1.1 The geographical position map of Tingnan Coal Mine



### 1.1.2 Mining technological conditions

---

#### 1) Lithology of coal seam roof and floor

No.4 coal seam roof in addition to the local area for medium and coarse grained sandstone, the other are mudstone, sandy mudstone with siltstone strip, 0.11 - 5.40 m thick, easy to fall, belongs to unstable hard roof, indirect roof is medium to fine grained sandstone, calcareous cementation, hard, one-way compressive strength 79.1 - 111.8 MPa, belongs to hard and stable roof.

The floor of No. 4 coal seam is grayish-brown bauxite mudstone, and the lower part contains oolitic particles, showing a massive structure. The floor swells when encountering water, and the floor heave occurs. The thickness is 1.13 – 7.89 m, and the unidirectional compressive strength is 18.2 – 68.6 MPa, belonging to the unstable and unstable medium-solid floor. The lithology of the lower stratum is siltstone, and the fractures are not developed. The unidirectional compressive strength is 98.8 MPa, which is considered to be a stable and strong rock according to the geological report.

#### 2) Gas

Due to the influence of coal-forming environment, the gas samples in No.4 coal seam are mainly nitrogen and gas, and the methane concentration is high, forming N<sub>2</sub>-CH<sub>4</sub> zone. The gas content in the north is higher than that in the south, and the absolute emission is 5 - 10 m<sup>3</sup>/min.

The basic law of gas content in No.4 coal seam: The gas content increases about 0.67 ml/g-daf when the depth of coal seam increases 100m. The methane content increases with the increase of methane concentration.

According to the gas identification results in 2014, the relative gas emission of the mine was 18.59 m<sup>3</sup>/t, and the absolute gas emission was 104.20 m<sup>3</sup>/min.

#### 3) Coal dust explosion risk

According to the latest identification results, the length of coal dust explosion flame is 400 mm, coal dust has explosion risk, the amount of anti-explosion rock powder is 65 %, and the explosion is strong.

#### 4) Coal spontaneous combustion

Before the mining of the fourth panel, the spontaneous combustion tendency of the coal seam is class II, which belongs to the spontaneous combustion coal seam. After the sampling and identification of the coal samples in the fourth panel, the spontaneous combustion tendency is class I, which belongs to the easily spontaneous combustion coal seam. The shortest spontaneous combustion period is 35 days.

---

### **1.1.3 Resources reserves**

---

No. 4 coal seam is the only recoverable coal seam in Tingnan Coal Mine. There are 60 boreholes in the whole mine field, 58 boreholes are located in No. 4 coal seam, which are all recoverable coal seams. The recoverable area is 29.95 km<sup>2</sup>, accounting for 84.25 % of the whole mine area.

Coal seam thickness 1.00 m (T14 hole) - 23.24 m (96 hole), average thickness 11.05 m. The thickness variation is obvious. Generally, the thickness of the uplift area is small, and the thickness of the depression area is large, which belongs to the coal seam with simple structure.

By the end of 2019, the reserves of Tingnan coal mine were 38.245 million tons and the remaining recoverable reserves were 21.262 million tons.

The annual working day of the mine is 300 days, three shifts per day, two shifts of production, one shift of preparation, and the net increase time of 14 hours per day.

---

### **1.1.4 Minefield development**

---

#### 1) Ways of field development

The mine adopts four opposite wells and single-level development. The No.4 coal seam in the minefield is a close to horizontal thick and extra thick coal seam (locally medium thick coal seam). The height difference between the shallow and deep coal seam floor in the minefield is only 165 m, so the single horizontal development is adopted. The horizontal elevation is + 455 m, which is basically in the middle of the inclined direction of the coal seam. The whole mine field is divided into four panel areas.

#### 2) Roadway layout and horizon selection

The mine level is set in No.4 coal seam. No.4 coal seam is the only minable coal seam in the mine field, and the whole mine field is stable. In the location of the main roadway, except the boundary of the mine field, most of the coal seam thickness is greater than 9 m. No. 4 coal seam is approximately horizontal, the maximum dip angle in the mine field is less than 7 °, and the maximum dip angle of the coal seam along the roadway is 3.5°. No. 4 coal seam has high hardness (unidirectional compressive strength 27.1 MPa, equivalent to 277.6 kg / cm<sup>2</sup>) and good supporting effect. At the same time, the belt conveyor is used as the main transportation, and the diesel engine rubber sleeve gear rail vehicle with strong climbing ability is used as auxiliary transportation. The roadway can be constructed according to the natural slope of the coal seam.

### 3) Panel division and mining sequence

According to the coal seam occurrence and mining technical conditions, the whole mine field is divided into four panel areas, two panel areas in the south of the roadway and two panel areas in the north of the roadway. Due to the small dip angle of the coal seam, the height difference between the shallow part and the deep part of the coal seam is not large, the second panel directly uses the western roadway mining, and the third and fourth panel separates the panel roadway mining.

The north-south length of the first panel is 1.8 km, the east-west width is 1.7 km on average, the recoverable reserve is 27.70 Mt, and the advancing length of the working face is 1.45 km. The second panel is located in the north of the main roadway. It is the panel with the best coal seam occurrence conditions and the thickest coal seam in the whole mine field. The length of the north and south is 1.9 - 2.5 km, the width of the east and west is 4.5 km, and the recoverable reserve is 68.01 Mt. The third panel is located in the south of the main roadway and the west of the first panel. The length of the north and the south is 0 - 1.8 km, the width of the east and the west is 2.0 - 4.6 km, the recoverable reserves is 29.40 Mt, the dip angle of the coal seam is large and the local is nearly 7 °, and the thickness of the coal seam changes greatly from 1.00 m to 11.40 m. It is a panel with the worst mining conditions in several panels. The fourth panel is located in the westernmost end of the well field, 1.3 - 2.0km long north and south, 1.5 - 2.1km long east and west, recoverable reserve is 25.1Mt.

According to the geological structure of the mine field and the occurrence characteristics of the coal seam, the mining is carried out in the order of the first, second, third and fourth panel areas according to the principles of shallowness first and then depth, nearness first and then distance, and high quality first and then the inferiors.

---

## **1.2 Research status**

---

### **1.2.1 Research status of coal spontaneous combustion mechanism**

---

According to the literature, in the 17th century, British Dr. Plott put forward the theory of pyrite genesis, and the study on the mechanism of coal spontaneous combustion began officially. Because coal contains many complex organic and inorganic substances, and its structure is very complex, so the research on the mechanism of coal spontaneous combustion has been continuing, so far there is no complete understanding of the reaction process of coal spontaneous combustion. In the past 400 years, with the continuous development of the research on the mechanism of coal spontaneous combustion, scholars and scientists have put forward many hypotheses on coal spontaneous combustion. The influential and recognized theories include coal-oxygen composite effect theory, bacterial gene theory and phenol gene theory (Zeng et al. 2006).

The theory of coal-oxygen interaction (Deng et al. 2003) has been supported by most scholars. Although the theory of coal-oxygen composite action is not perfect, it has been able to explain most of the phenomena in coal spontaneous combustion, and has also played a very good guiding role in the engineering application practice of mine fire prevention. The theory of coal-oxygen composite action is based on the combination of solid coal and gas phase oxygen. In the process of combination, complex physical adsorption, chemical adsorption and chemical reactions occur, and oxidation exothermic occurs. This reaction is accelerating under spontaneous combustion. The heat release and heat dissipation of coal and oxygen in the combination process are a pair of contradictory effects at the same time. When the heat release is greater than the heat dissipation, the heat begins to accumulate, and to a certain extent, it will eventually lead to coal spontaneous combustion.

Conversely, heat dissipation is greater than heat release, which will lead to coal weathering.

The research on low-temperature oxidation of coal is an exploration of the theory of coal-oxygen interaction (Wang et al.1999). As a complex mixture, coal not only contains a variety of organic and inorganic substances, but also has developed pore structure and large specific surface area. Coal oxidation occurs not only on the surface of coal, but also in the internal pores of coal.

The low temperature oxidation process of coal can be divided into four stages(Lu et al. 2009): (1) oxygen in air diffuses to or is adsorbed to the inner and outer surface of coal ; (2) Oxygen combines with the active position of coal surface to form unstable intermediate products; (3) Intermediates decompose and release H<sub>2</sub>, CO, CO<sub>2</sub>, H<sub>2</sub>O, CH<sub>4</sub> and other hydrocarbon gases;(4) After the decomposition of intermediate products, a new surface is exposed, coal and oxygen are combined again, and this process will be recycled. In this process is also accompanied by heat production and cooling process. The most important stage is the combination of oxygen and coal surface active position, which plays a decisive role in the low temperature oxidation process of coal, and this process is affected by various factors.

---

### **1.2.2 Research status of coal spontaneous combustion prevention**

---

There are three main aspects of the prevention and control of coal spontaneous combustion: Before the occurrence of spontaneous combustion, make a scientific risk assessment of coal spontaneous combustion. Early warning of possible coal spontaneous combustion. Take fire-fighting measures against imminent or already occurring spontaneous combustion (Chen et al. 2009).

The tendency of coal seam spontaneous combustion, that is, the difficult state of coal seam spontaneous combustion, is the embodiment of whether coal is easy to be oxidized, and is one of the essential attributes of coal. The fire prevention and extinguishing grade of mine is mainly divided according to the spontaneous combustion tendency of coal seam(Wang et al. 1990). In China, the physical oxygen absorption method is mainly used to identify the spontaneous combustion tendency of coal, that is, the chromatographic oxygen absorption identification method (Lu Wei 2008).

Since the 1950s, China has adopted grouting fire-fighting technology in coal mines. From the 1960s to the 1970s, coal mines began to adopt pressure-equalized ventilation fire-fighting technology, foam fire-fighting technology and inhibitor fire-fighting technology. From the 1980s to the 1990s, China started to adopt inerting fire-fighting technology, gel fire-fighting technology, and leak-stopping wind fire-fighting technology. Since then, scientific research workers have improved the performance of the original technology and developed new fire prevention materials (Liang et al. 2008).

Mine fire-fighting is a complex system engineering. Only by continuously strengthening basic theoretical research and development of new technologies, focusing on practice and innovation, and combining multi-disciplinary knowledge, can coal mine fire-fighting be more effectively achieved.

---

### **1.2.3 Research status of research on prediction and forecast technology of coal spontaneous combustion**

---

At this stage, there are four main types of predictions for coal spontaneous combustion: index gas analysis method, temperature measurement method, tracer gas method and odor detection method.

The index gas analysis method means that in the low-temperature oxidation process of coal, a series of gases reflecting the oxidation status will be produced as the reaction process progresses, such as: CO, CO<sub>2</sub>, H<sub>2</sub>, CH<sub>4</sub>, C<sub>2</sub>H<sub>6</sub>, C<sub>2</sub>H<sub>4</sub>, C<sub>2</sub>H<sub>2</sub>, etc. The output of various index gases varies significantly with the reaction temperature, and the development stage of coal spontaneous combustion can be judged according to the generation of index gases (Luo et al. 2003). In recent years, many scholars have proposed the use of alkanes and olefins as index gases for early warning of coal spontaneous combustion. At the same time, a paraffin ratio analysis method that combines alkanes and olefins has emerged. The sensitivity of monitoring has been significantly improved, and the index gas has also been formed. A new method based on compound calculation results.

Temperature measurement method refers to the use of temperature sensors to monitor the temperature of some points in the coal seam in real time, and to analyze the temperature to determine the prediction method of the coal fire risk (Zhang et al. 2005).

The tracer gas method uses a combination of a gas with good thermal stability and a gas that is easily decomposed by heat, and releases the two gases at the same time in the same environment, and then collects the gas at the monitoring point for comparative calculation and analysis, thereby monitoring the ground leakage in the area and temperature value (Cui et al. 2001).

In the odor detection method, the odor sensor can detect the subtle changes in the odor released at the initial stage of low-temperature oxidation of coal, and can sense this change at 30-40°C. The odor detection method uses a group of different types of odor sensors, according to the difference in the frequency of the crystal oscillator device caused by the sensor's bionic bimolecular membrane after receiving odor stimulation, and based on the artificial neural network theory, to identify different odor substances, so as to achieve early warning of coal spontaneous combustion (Yang et al. 2007).

## **2 Study on the mechanism of coal seam spontaneous combustion**

---

### **2.1 Transport and adsorption of oxygen in coal**

---

The oxidation and spontaneous combustion of coal mostly occurs in the loose coal. When the air penetrates into the loose coal, the oxygen in the air comes into contact with some active structures on the surface of the coal molecules, and complex physical and chemical effects occur under normal temperature and pressure. Under certain heat storage conditions, the heat released causes the temperature of the coal body to continue to rise, which eventually leads to the occurrence of spontaneous combustion (Deng et al.2003).

According to the principle of coal-oxygen compounding, coal spontaneous combustion is a process in which coal adsorbs oxygen (Wang et al. 2014) . Coal is a kind of porous material. The original solid coal adsorbs CH<sub>4</sub> and other gases and moisture. During the whole process of changing from the original coal body to loose coal under the action of external force, under the action of the concentration difference, CH<sub>4</sub> and other gases and water The water will desorb. The granular coal particles have a large specific surface area, and there are a variety of active sites on the surface, which have a strong adsorption capacity for oxygen. When oxygen diffuses to the surface of the granular coal, the surface of the granular coal continuously adsorbs oxygen. In the process of physical and chemical adsorption, heat is released, and under the conditions of difficult heat dissipation, heat accumulation causes spontaneous combustion of coal.

The oxygen adsorbed in the coal pores will go through these processes: the oxygen diffused into the coal passes through the stagnant membrane layer around the particles, and is transmitted to the outer surface of the coal particles in the form of molecular diffusion and convective diffusion; the oxygen merges from the outer surface of the coal particles. It diffuses into the inside of the particles through the



upper micropores and reaches the inner surface of the particles; oxygen is adsorbed on the inner surface of the coal pores (You et al. 2018).

Equation 2.1 is the adsorption equation of oxygen on the surface of coal in the process of coal-oxygen recombination.  $P$  is the partial pressure of oxygen in the process of coal-oxygen recombination, and  $\mu$  is the number of moles of oxygen impinging on the carbon surface of  $1 \text{ cm}^2$  per second, and it is assumed to be proportional to the partial pressure  $P$  of oxygen, and  $a$  is the scale factor.

$$\mu = a P \quad 2.1$$

If a part of the oxygen moles impacting on the carbon surface is adsorbed, then the number of moles of oxygen adsorbed on the carbon surface per square centimeter is  $a\mu$ .

If it is assumed that the ratio of the surface covered by oxygen molecules to the total surface area is  $\theta$ , the proportion of free surface not covered by oxygen molecules is  $(1-\theta)$ . Therefore, the adsorption rate of oxygen is:

$$W_a = (1-\theta) a \mu \quad 2.2$$

But at the same time, some oxygen molecules will leave the carbon surface. The rate at which oxygen molecules detach,  $W_b$ , is proportional to the surface area covered by oxygen molecules, and  $v$  is the scale factor, that is:

$$W_b = v\theta \quad 2.3$$

When the speed at which oxygen molecules are adsorbed is equal to the desorption speed, the adsorption equilibrium is reached. at this time:

$$(1-\theta) a \mu = v\theta \quad 2.4$$

From the above formula:

$$\theta = \frac{a\mu}{v + a\mu} \quad 2.5$$

Substituting  $\mu = aP$  into the above formula:

$$\theta = \frac{k_1 p}{1 + k_1 p} \quad 2.6$$

Suppose  $k_1 = \frac{\alpha a}{v}$  (called the adsorption constant), then the above formula can be written as:

$$\theta = \frac{k_1 p}{1 + k_1 p} \quad 2.7$$

If the total surface area of carbon particles is  $n\text{cm}^2$  and the amount of oxygen adsorbed per unit area on the oxygen-covered surface is  $Y\text{g}$ , then the total amount of oxygen adsorbed on the carbon surface is:

$$x = Yn\theta \quad 2.8$$

Therefore

$$x = \frac{Ynk_1 p}{1 + k_1 p} = \frac{k_1 k_2 p}{1 + k_1 p} \quad 2.9$$

Where,  $k_2 = Yn$ ,

This formula is the Langmuir isotherm adsorption equation.

Fig. 2.1 shows the diagram of this equation:

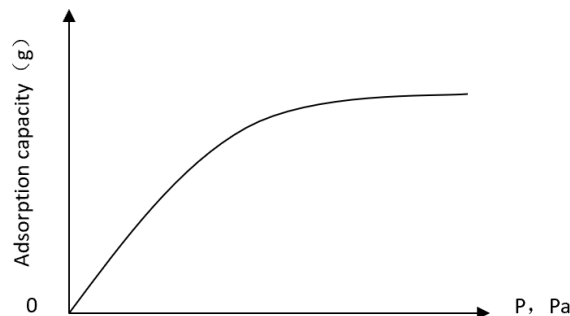


**Fig. 2.1 Langmuir adsorption isotherm**

The analysis of formula 2.8 and 2.9 is as follows:

When the carbon surface has a weak ability to adsorb oxygen, that is, the adsorption coefficient  $k_1 \ll 1$ , there is

$$x = k_1 k_2 p = k_2 p, \theta = k_1 p \quad 2.10$$

That is, the amount of oxygen adsorbed on the surface is proportional to the partial pressure of oxygen. This relationship corresponds to the initial part of the diagonal line that intersects the origin of the ordinate on the adsorption isotherm.

When the carbon surface has a strong ability to adsorb oxygen, that is, the adsorption coefficient  $k_1 \gg 1$ , there is

$$x = \frac{k_1 k_2 p}{k_1 p} = k_2, \theta = 1 \quad 2.11$$

At this time, the amount of oxygen adsorbed on the surface has reached the limit and cannot be increased later, that is, the entire carbon surface has been covered by adsorbed oxygen molecules. This relationship corresponds to a straight line parallel to the abscissa in the figure above.

Therefore, it can be considered that the speed of the heterogeneous reaction is proportional to the solid surface covered by the adsorbed molecules, that is, the larger the covered surface area, the greater the adsorption capacity and the faster the reaction speed. This can be expressed as:

$$\frac{dx}{dt} = k' \theta \quad 2.12$$

When the carbon adsorption capacity is very weak,  $\theta = k_1 p$ , so

$$\frac{dx}{dt} = k' \theta = k' k_1 p \quad \text{or} \quad \frac{dx}{dt} = k = k \theta \quad 2.13$$

When the reaction rate is related to the partial pressure (or concentration) of oxygen. In this case, it is a single-molecule reaction, and the number of reaction stages is 1.

When the carbon adsorption capacity is very strong,  $\theta = 1$ , then there is

$$\frac{dx}{dt} = k' \theta = k' \quad 2.14$$

When the reaction rate has nothing to do with the partial pressure (or concentration) of oxygen, the carbon-oxygen heterogeneous reaction is zero-order reaction. When the reaction is between the above two extreme situations, there are:

$$\frac{dx}{dt} = k' p^n \quad 2.15$$

$$n = \frac{1}{m}, m > 1 \quad 2.16$$

At this time, the order of the carbon-oxygen heterogeneous reaction is a fraction, that is,  $n$  is between 0 and 1.

---

## 2.2 Heating and burning of coal

---

### 1) Heating of coal on fire

#### (1) Critical conditions for judging the ignition point

Due to the effect of oxygen on the surface of coal, coal particles can react slowly, leading to spontaneous combustion of coal. The variables that affect the ignition temperature and ignition time of coal include: coal type, volatile content, gas composition, coal particle size, coal moisture content, coal particle size distribution, gas temperature, coal concentration or quality, surface temperature, gas velocity, percentage of mineral impurities, etc (Yang 2015, Fei 2019) .

The ignition of coal can be based on Semenov thermal ignition theory. The ignition point can be judged by the critical condition :

$$Q_1 = Q_2, \frac{dQ_1}{dT} = \frac{dQ_2}{dT} \quad 2.17$$

The calculated thermal ignition temperature is the temperature of coal particles and surrounding gas at the critical ignition point.

#### (2) Semenov theory of thermal ignition

For example, if there is a container with a volume of  $V$  ( $m^3$ ), which is filled with a chemically homogeneous combustible mixture, its concentration is  $C$  ( $kg/m^3$ ), the

original wall temperature of the container is  $T_0(K)$ , and the combustible gas mixture in the container is moving at a speed  $\omega$  ( $kg /m^3 \cdot s$ ) During the chemical reaction, part of the heat released after the chemical reaction heats the gas mixture to increase the temperature of the reaction system, and the other part is transferred to the surrounding environment through the container wall.

In order to simplify the calculation, Semenov adopted the "zero-dimensional" scheme, which does not consider the distribution of the temperature, the concentration of reactants and other parameters in the container, but calculates all the parameters in the entire container as the average value, that is, assuming:

The concentration and temperature of the mixture are the same everywhere in the container.

During the reaction, the reaction speeds are the same everywhere in the container.

The wall temperature  $T_0$  of the container and the temperature of the external environment remain unchanged during the reaction, and the temperature difference that determines the heat transfer intensity is the temperature difference between the wall temperature and the mixture.

In the vicinity of the ignition temperature, the change in the concentration of the combustible gas mixture caused by the reaction is negligible.

If is expressed in unit time due to the heat released by the chemical reaction, then

$$Q_1 = \omega qV \quad 2.18$$

In the formula,  $\omega$ —chemical reaction rate,  $kg/(m^3 \cdot s)$

$q$ —The thermal effect of chemical reaction,  $J/kg$

$V$ —Volume of container,  $m^3$

The chemical reaction speed  $\omega$  is:

$$\omega = k_0 e^{-E/RT} C^n \quad 2.19$$

If the reaction order  $n=1$ , then

$$\omega = k_0 e^{-E/RT} C^n \quad 2.20$$

Therefore,

$$Q_1 = qV k_0 e^{-E/RT} C \quad 2.21$$

Let  $A = qV C k_0$ , by the above assumptions, and A is a constant, then

$$Q_1 = A e^{-E/RT} \quad 2.22$$

The heat  $Q_2$  transferred from the container to the surrounding environment in unit time is:

$$Q_2 = aF(T - T_0) \quad 2.23$$

Where, a-surface heat transfer coefficient,  $W(m^2 \cdot K)$

F-surface area of the container,  $m^2$

T-The temperature of the mixture in the container at a certain moment, K

$T_0$ -container wall temperature, K

The surface heat transfer coefficient a is related to the shape, size and material of the container. For a container of a certain shape and size,  $aF$  is a constant. Let  $B = aF$ , then the above formula can be written as

$$Q_2 = B(T - T_0) \quad 2.24$$

As shown in Fig. 2.2,  $Q_1$  represents an exponential curve,  $Q_2$  is a straight line under different conditions, and its slope is  $aF$ . The analysis of three different heat dissipation intensities is as follows:

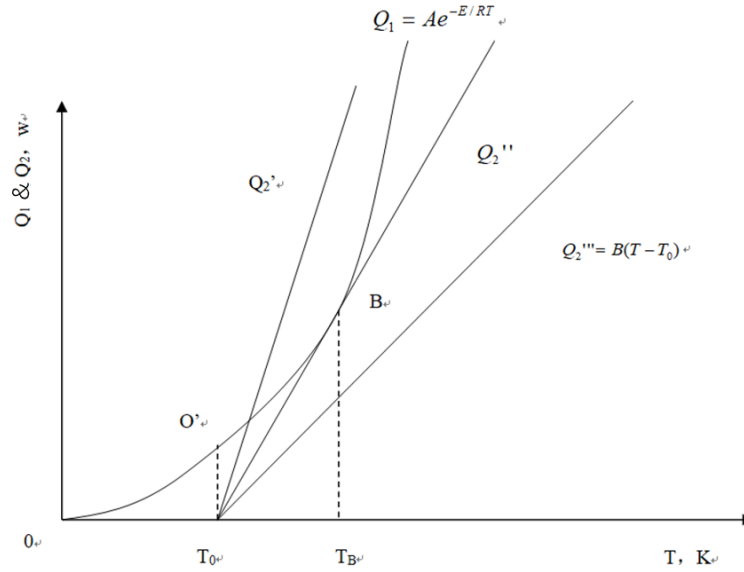


**Fig. 2.2 The relationship between chemical reaction heat release and convective heat dissipation and temperature**

① When the heat dissipation intensity is great, that is, the straight line  $Q_2'$  in the figure.

As the chemical reaction of the combustible mixture in the container continues to increase the temperature, it can be seen that the heat released by the combustible increases with the increase in temperature in an exponential relationship, and the heat dissipation increases with the increase in temperature. At the beginning, the temperature is very low, and the heat released by the reaction is greater than the heat released, so the temperature in the container rises, and as the temperature rises, the heat released is greater than the heat released, making the state return to the beginning. In this state, the general fuel hardly changes in a limited time.

② When the heat dissipation intensity is very small, such as the straight line  $Q_2'''$  in the figure.

In this case, the heat emitted by the reaction will always be greater than the heat emitted, and the temperature in the container will continue to increase, and the chemical reaction will accelerate with the increase in temperature, which will cause the combustibles to deflagrate.

③ When the heat dissipation intensity is carried out according to the straight line of  $Q_2''$  in the figure.

Starting at temperature  $T_0$ , the heat emitted by the reaction is greater than the heat emitted, and the temperature of the combustible mixture in the container continues to rise. When the temperature rises to point B, the heat dissipation line is exactly tangent to the heat release curve, and the reaction emits the heat is exactly equal to the heat dissipated. But point B is also unstable. If the heat dissipation is slightly less, the combustibles will be directed to the high-temperature area, the reaction will accelerate and deflagration will occur. On the contrary, if there is a little more heat dissipation, the reaction will always stay in the low-temperature oxidation zone. Therefore, point B in the critical state is called the ignition point, and its corresponding temperature is called the ignition temperature.

## 2) Combustion Process of Coal

Taking coal as the main body to describe the combustion process of coal. First, the coal particles are heated and dried to above  $10^\circ\text{C}$  by external energy. After the moisture in the coal gradually evaporates, as the temperature increases, volatiles are precipitated to form coal char. After reaching the ignition temperature, the volatiles and coal char ignite, and finally, the minerals in the coal turn into ash. The above processes may occur sequentially under the condition that the combustion space is sufficient, and may intersect with each other or synchronously when the combustion space is insufficient or the coal is continuously added.

### (1) Single coal particle model

#### ① Heating of coal

When the coal particles are heated, the energy equation is:

$$Q_p = m_p \frac{di_p}{dt} - \frac{dm_p}{dt} (h_s - h_p) \quad 2.25$$

In the formula:  $Q_p$  - the heat transfer rate of the environment to the particles;



$i_P$  - particle enthalpy;

$m_P$  - the mass of the particle;

$h_P$  - particle specific enthalpy;

$h_s$  - specific enthalpy of particle surface.

The  $Q_P$  includes two parts: convective heat transfer  $Q_{PC}$  and radiation heat transfer  $Q_{PR}$ , namely:

$$Q_p = Q_{pc} + Q_{pr} \quad 2.26$$

## ② Water evaporation model

Usually, the moisture in the pulverized coal has been precipitated during the drying and pulverizing process, but there may still be some coal particles with high moisture content. The evaporation of water in coal is generally limited by diffusion and can be described as:

$$\dot{m}_w = \frac{M_w Nu_{im} C_g D_{wm} n_i A_j (x_{wj} - x_{wg})}{Nu_{im} d_j \left(1 - \frac{x_{wj} \dot{m}}{\dot{m}_w}\right)} \quad 2.27$$

The temperature of coal particles is much lower than the boiling point of water. Radiation and convective heat transfer of coal particles during continuous heating may limit the evaporation rate of water:

$$(\dot{m}_w)_{\max} = \frac{Q_j + Q_{fj}}{\Delta h_w} \quad 2.28$$

## (2) Volatile precipitation model

There are many models for the precipitation of volatiles, but the ideas of most models are the same, but the depth of understanding and mathematical expression are different. The main assumptions are: A pulverized coal particles are spherical; B particles have a uniform temperature, the properties of each part are the same,

the volatilization process is the same, and it is not affected by the region. The main models are:

① Single equation model (Badzioch et al. 1970)

$$\frac{dV}{dt} = K(V_{\infty} - V) \quad 2.29$$

$$K = A \exp(-E/RT) \quad 2.30$$

$$V_{\infty} = Q(1 - V_c)V_p \quad 2.31$$

Among them, Q, V<sub>c</sub>, etc. are determined by experiments, and the method is relatively simple. In fact, V<sub>p</sub>, K, Q, V<sub>c</sub>, and E depend on the specific pulverized coal species, thus limiting the generality of this model.

② Double equation model (Frazier G C et al. 1982)

This is an idea to describe the volatile precipitation process of coal with two parallel first-order reactions, that refers the pyrolysis of coal is governed by two competing parallel reactions. The formula of the reaction process is:

$$\frac{dv}{dt} = \frac{dV_1 + dV_2}{dt} (a_1 K_1 + a_2 K_2) \quad 2.32$$

$$\frac{dC}{dt} = -(K_1 + K_2)C \quad 2.33$$

Where, C is the percentage of unreacted coal remaining in the char.

K<sub>1</sub>, K<sub>2</sub> are Arrhenius-type constants:

$$K_1 = K_{10} \exp(-E_1/RT) \quad 2.34$$

$$K_2 = K_{20} \exp(-E_2/RT) \quad 2.35$$

Where, E<sub>1</sub> < E<sub>2</sub>.

This reaction means that the precipitation of volatiles in coal has two peak states, one is dominated by low temperature and the other is dominated by high

temperature. Using this model, the processing of many experimental data has obtained satisfactory results, so it has obtained more applications.

### ③ Precipitation model of multicomponent volatiles

There are various components in coal, and their precipitation also has different rules. Therefore, a volatilization model is proposed for each component, as follows:

$$W_i = W_i^0 (1 - \exp(-K_k T)) \quad 2.36$$

$$K_i = A_i \exp(-E_i/RT) \quad 2.37$$

In the formula,  $i$  is the  $i$ -th volatile component.

Solomon (Solomon et al. 1988) uses the method of spectral analysis to analyze the composition of coal, and believes that as long as it contains the same component, there is the same precipitation law for any coal type, so it has the possibility of being universal.

### (3) Volatile components

Although the volatilization kinetic model describes some features of the volatilization process, it still does not describe the whole volatilization process. The reason for this is that the characterization of the products released from coal is difficult. The aforementioned dynamic models are partly involved in this issue, and most pulverized coal combustion models must also have a part about volatile components, and this part is generally determined by one of the following methods, namely:

- ① The composition of the residue (fixed carbon and ash) is specified, and the composition of the volatile matter is determined by the material balance method and the analysis of the raw coal. The gas composition and temperature can be specified in detail with the corresponding local equilibrium calculations.
- ② The volatile substances and components are based on the experimental results summarized by the experience of the volatile products in the decomposition experiments. This product will eventually be reacted in the total rate control process

of the gas phase. When the coal particles are gradually consumed, carbon can be used. The experimental data of hydrogen, oxygen, nitrogen and sulfur are used to evaluate the change of volatile components of coal.

## 3 Experimental Study

---

### 3.1 Introduction to the experimental device

---

In order to analyze the combustion characteristics of coal spontaneous combustion, the thermogravimetric-Fourier infrared analysis method was used to study the functional groups of coal, the stage thermogravimetric characteristics of coal in the pyrolysis process, and the infrared characteristics of characteristic gases. Reaction kinetic parameters. At the same time, by analyzing the characteristic gases produced by thermal decomposition of coal and the functional groups of coal, the structure of functional groups inside Tingnan coal is obtained.

The structure of coal is complex and changeable, but some groups with oxidative activity in the coal determine the spontaneous combustion tendency of coal. By analyzing and comparing the content of oxidative active groups in the coal, the oxidizing power of the coal can be judged, that is, the spontaneous combustion tendency of the coal. At present, infrared spectroscopy is one of the most commonly used methods to study the functional group structure of coal. When irradiated with infrared light, different functional groups have their characteristic absorption peaks at different wavelengths, so the application of infrared spectrum analyzer can not only determine the type of functional groups in coal, but also determine its content.

In the process of coal pyrolysis and combustion, the structure of coal and the oxygen-containing functional groups in coal have a great influence on the decomposition of coal. Fourier transform infrared spectroscopy was used to study the structure and functional groups of coal for different coal samples, and synchronous thermal analyzer and Fourier transform infrared spectrometer were used to study the gases decomposed by thermal decomposition of coal. The experimental apparatus is shown in Fig. 3.1 (a), (b)

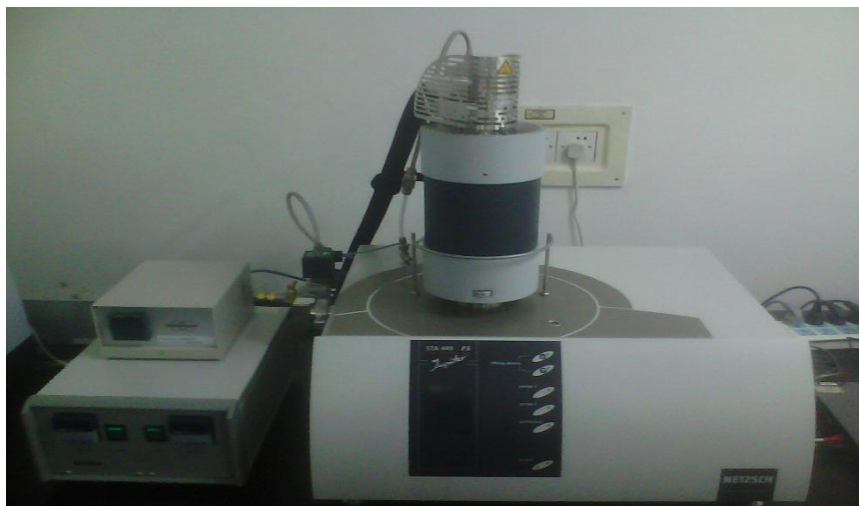


Fig. 3.1(a) Synchronous thermal analyzer



Fig. 3.1(b) Fourier Transform Infrared Spectrometer

---

## 3.2 Principle of the experiment

---

### 3.2.1 Thermo Gravimetric Analysis (TGA)

---

The Thermo Gravimetric Analysis measures the relationship between sample quality and temperature through program temperature control (Dong et al. 2011). When the coal sample undergoes oxidation, dehydration and decomposition during the heating process, its quality will change accordingly. Using a synchronous thermal analyzer, record the corresponding relationship

between the temperature and the quality of the coal sample in the process of programmed heating, and obtain the thermo gravimetric line diagram of the coal sample, as shown in the curve (a) in Fig.3.2.

The derivative thermogravimetric method (DTG) derived from the thermogravimetric method is the first derivative of the TG curve with respect to temperature (or time). That is, plot the change rate of coal sample quality ( $dm/dt$ ) against temperature  $T$  (or time  $t$ ) to obtain the DTG curve, as shown in the curve b in Fig.3.2.

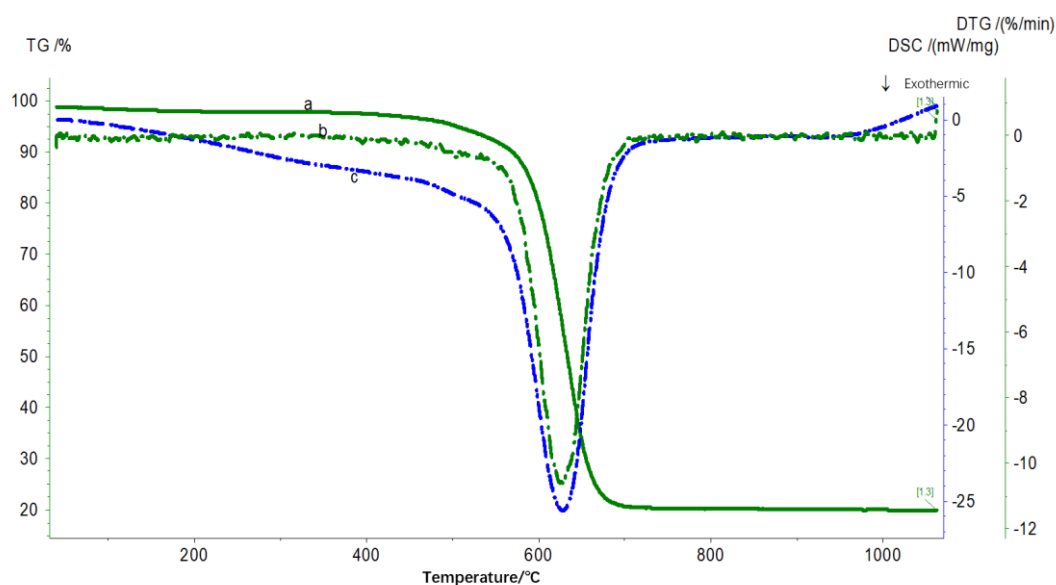
---

### **3.2.2 Differential Scanning Calorimetry (DSC)**

---

Differential Scanning Calorimetry is to measure the relationship between the energy difference between the sample and the reference and the temperature change through temperature programming. Differential scanning calorimetry has two methods: compensation method and heat flow method. It is mainly used to measure various thermodynamic and kinetic parameters (Landry, M. R. 2005).

The curve of the relationship between the applied heat and the temperature required to keep the temperature difference between the sample and the reference at zero per unit time is called the DSC curve, as shown in Fig.3.2. The vertical axis of the curve is the amount of heating per unit time, and the horizontal axis is temperature or time. The area of the curve is proportional to the change in enthalpy. DSC test has the advantages of wide temperature range, good resolution, sensitivity and reproducibility. Therefore, DSC test has been widely used in the polymer field.

**Fig.3.2 TG-DSC curve**

### 3.2.3 Fourier Transform Infrared Spectroscopy (FTIR)

Infrared spectroscopy studies the relative vibration of atoms in molecules, or the vibration changes of chemical bonds. Different chemical bonds (functional groups) require different energy levels to transition from the ground state to the excited state. Therefore, different infrared light energies must be absorbed and different absorption peaks appear in the instrument to form an infrared spectrum (Qiao, et al. 2016).

## 3.3 Influencing factors of the experiment

### 3.3.1 Influencing factors of thermogravimetric experiments

The experimental results of thermogravimetric analysis are affected by many factors, including instrumental factors and sample factors. In the measurement of thermogravimetric experiments, too fast heating rate will significantly increase the decomposition temperature of the sample (Zhang et al. 2011).

During the heating process of the sample, there will be endothermic and exothermic phenomena, so that the temperature deviates from the linear



heating program, thereby changing the position of the thermogravimetric curve. The greater the sample mass, the greater this effect. The particle size should not be too small, otherwise both the starting temperature of decomposition and the temperature at which decomposition is completed will decrease. In short, the sample volume should be adjusted according to the sensitivity of the balance during the experiment.

---

### **3.3.2 Influencing Factors of Differential Scanning Calorimetry Experiments**

---

Sensitivity and resolution are a pair of contradictions. The sample volume is small, the resolution is high, and the sensitivity is reduced. Generally, the sample amount is adjusted according to the size of the thermal effect of the sample, generally 3 to 5 mg. On the other hand, the sample size also has an effect on the temperature. With the increase of sample amount, the peak onset temperature remained basically unchanged, but the peak top temperature increased and the peak end temperature also increased. Therefore, it is best to use the same amount when comparing similar samples to each other.

The temperature rise rate is usually in the range of 5 to 200°C/min. Generally speaking, the faster the heating rate, the higher the sensitivity and the lower the resolution. One generally chooses a slower heating rate to maintain good resolution, but increases the sensitivity by increasing the sample mass. Typically, as the heating rate increases, the melting peak onset temperature does not change much, but the peak top and peak end temperatures increase and the peak shape broadens.

Generally, the use of inert gases, such as nitrogen, argon, helium, etc., will not produce oxidation peaks, and at the same time, it can reduce the corrosion of the monitor by the sample volatiles. The airflow rate must be constant (eg 10ml/min), otherwise it will cause baseline fluctuations. The properties of the gas have a significant effect on the determination and should be noted. For

example, the thermal conductivity of helium is nearly 4 times larger than that of nitrogen and argon, so when using helium as a protective gas for low-temperature DSC experiments, the cooling speed is accelerated and the measurement time is shortened, but because of the thermal conductivity of helium The high rate reduces the detection sensitivity of the peak, which is about 40% of that of nitrogen. Therefore, when measuring heat in helium, it must be re-calibrated with a standard material for approval. When measuring in air, pay attention to the effect of oxidation. Some oxidation reactions can sometimes be explained by comparing the DSC curves in nitrogen and oxygen.

---

### 3.3.3 Influence Factors of Fourier Transform Infrared Spectroscopy

---

Influence from the operator: ① Differences in the selection process: the number of standard samples; the selection of standard samples; the accuracy of basic data analysis. ② Sample pretreatment method: sample preparation method; sample uniformity; ③ sample storage method; ④ sample loading difference. Influence from samples: ① Mutual interference between components; ② Influence of chemical components on physical properties; ③ Moisture content of materials; ④ Temperature of samples and test environment; environment. Influence from the instrument: ① wavelength accuracy; ② spectral resolution; ③ wavelength reproducibility; ④ temperature control system; ⑤ stability of power supply; ⑥ software processing function(Wu. 1994).

---

### 3.3.4 Experiment Procedure

---

The Tingnan coal was immediately put into a plastic bag and sealed, transported to the laboratory and placed in the refrigerator. During the experiment, open the sealed bag and pulverize the large coal into the required particle size for the experiment. Experimental steps: ① Sample preparation and inspection circuits. ② Weigh. ③ Set the temperature program. ④ Vacuum and inflate. ⑤ Start the temperature program, the coal sample releases

gas.⑥Transmission of temperature-programmed images, FTIR detection.⑦Data analysis.

---

### **3.4 Analysis of coal thermo gravimetric analysis**

---

#### **3.4.1 Influence of oxygen concentration on coal thermo gravimetric experiment**

---

Compare and analyze the TG, DTG, DSC curves of coal samples when the particle size  $<0.178\text{mm}$ , heating rate  $10\text{ }^{\circ}\text{C}/\text{min}$ , and different oxygen concentrations. The results are shown in Fig.3.3 (a), (b), (c).

It can be seen from Fig.3.3 that the curve of thermal decomposition of coal shifts to the low temperature direction when the oxygen concentration is increased. This is due to the increase in oxygen concentration, the shortening of the time for the physical and chemical adsorption of coal and oxygen to reach equilibrium, and the increase in the ability of coal's specific surface area to combine with oxygen per unit time, so the pore oxygen absorption of coal is in the unit If the time is also increased, the oxidation reaction rate of coal will be accelerated, the temperature value and the maximum weight loss rate value when reaching the burn-out point will be reduced, and the spontaneous combustion time of coal will be shortened, that is, the thermogravimetric curve will move forward.

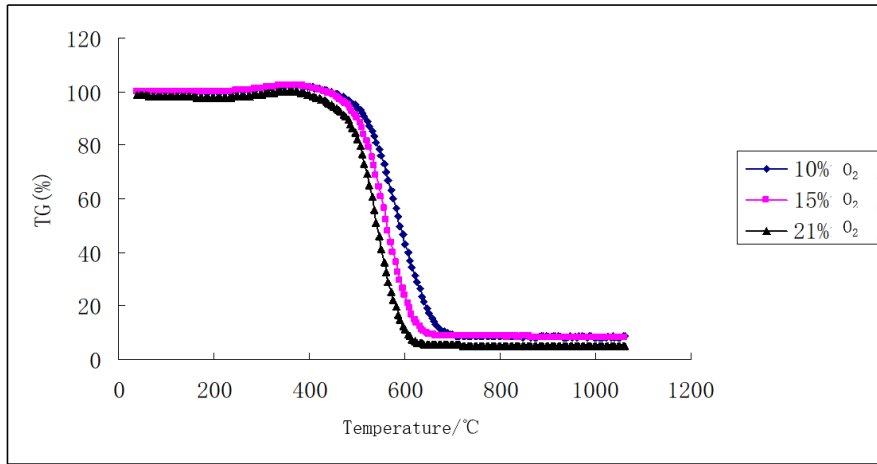


Fig.3.3(a) Influence of different oxygen concentration on coal TG curve

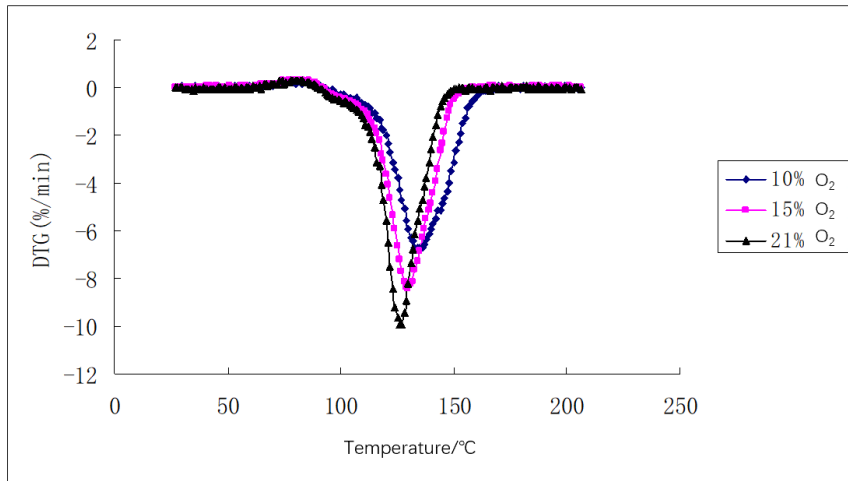


Fig.3.3(b) Influence of different oxygen concentration on coal DTG curve

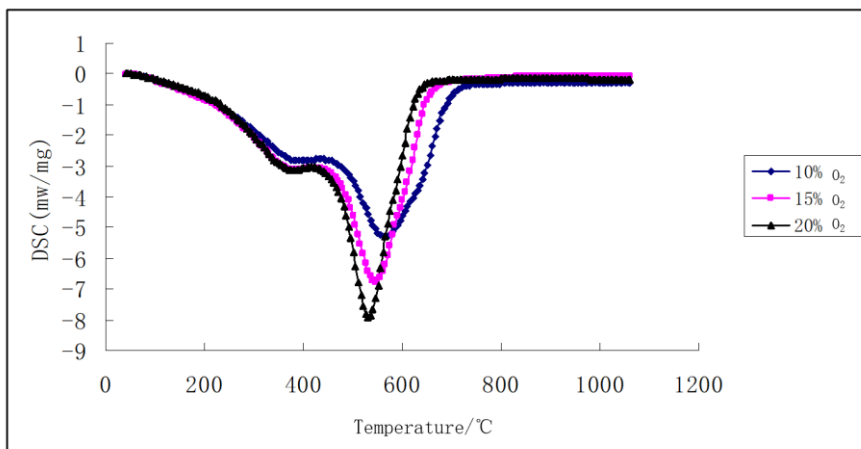


Fig.3.3(c) Influence of different oxygen concentration on coal DSC curve

### 3.4.2 Influence of heating rate on coal thermo gravimetric experiment

Compare and analyze the TG, DTG, and DSC curves of coal samples when the particle size and oxygen concentration are constant and the heating rate is changed. The results are shown in Fig.3.4(a), (b), (c).

It can be seen from Fig.3.4 that as the heating rate increases, the TG and DSC curves of coal have a hysteresis, while the DTG curve moves forward and the rate increases. This is because the coal gasification reaction when heated is an endothermic reaction, but the thermal conductivity of coal is poor, and it takes a certain amount of time for the reaction to proceed and the product to precipitate. With the increase of the heating rate, the time required for tar cracking will be shortened, the total amount of tar will increase, and part of the structure is not completely cracked, which causes the product to escape and drift towards high temperature, resulting in a hysteresis phenomenon. At the same time, the heating rate is relatively large. After the coal enters the combustion reaction stage, the combustion reaction will release a certain amount of heat to the environment. It is difficult to ignite the coal when the coal sample's self-reaction heat minus the remaining heat generated by the environment. When the components are burned, the curve changes will appear to slow down as the temperature rises.

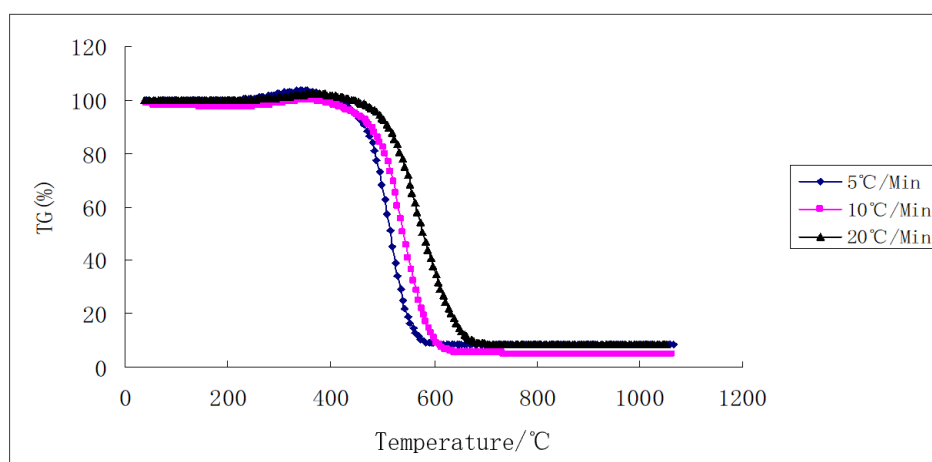
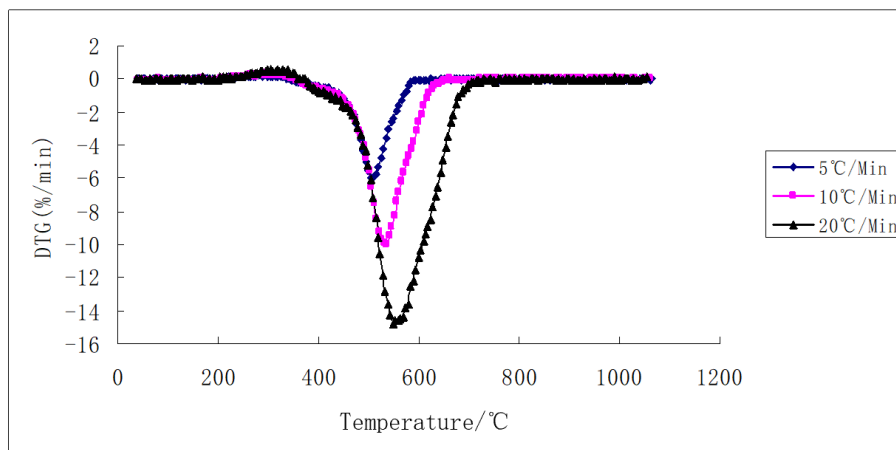
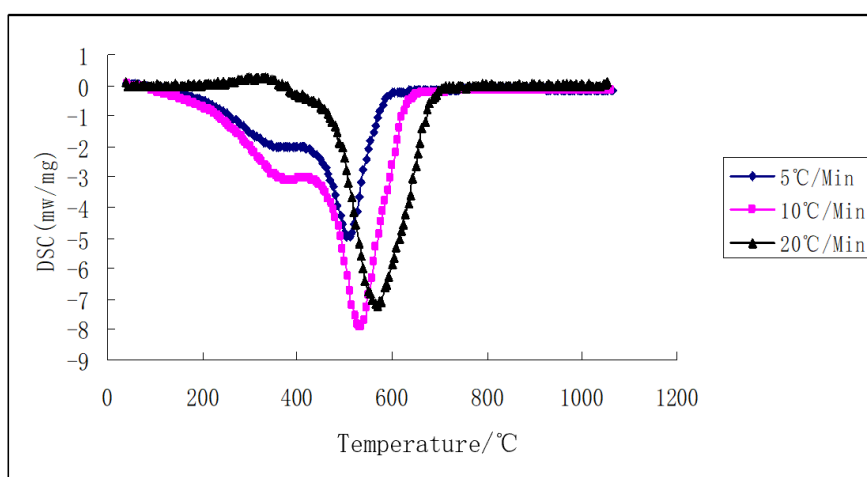


Fig.3.4(a) Influence of different heating rate on coal TG curve



**Fig.3.4(b) Influence of different heating rate on coal DTG curve**



**Fig.3.4(c) Influence of different heating rate on coal DSC curve**

### 3.4.3 Influence of particle size on coal thermo gravimetric experiment

Compare and analyze the TG, DTG, DSC curves of coal samples when the heating rate is 10°C/min, the oxygen concentration is 21%, and the particle size(mesh) is different. The results are shown in Fig.3.5 (a), (b), (c).

It can be seen from Fig.3.5 that as the particle size becomes smaller, the TG, DTG, and DSC curves move forward, the maximum combustion weight loss rate value of coal increases, the ember temperature value decreases, and the total time of coal oxidation and spontaneous combustion is shortened. That is, the larger the particle size of the coal sample, the longer the oxidation time of

the coal, the smaller the spontaneous combustion tendency, and the harder it is to ignite spontaneously.

This is because the smaller the particle size, the larger the specific surface area, and the larger the contact area with air, the greater the oxidation reaction speed, and the oxidation will reduce the size of coal particles, further shortening the reaction time.

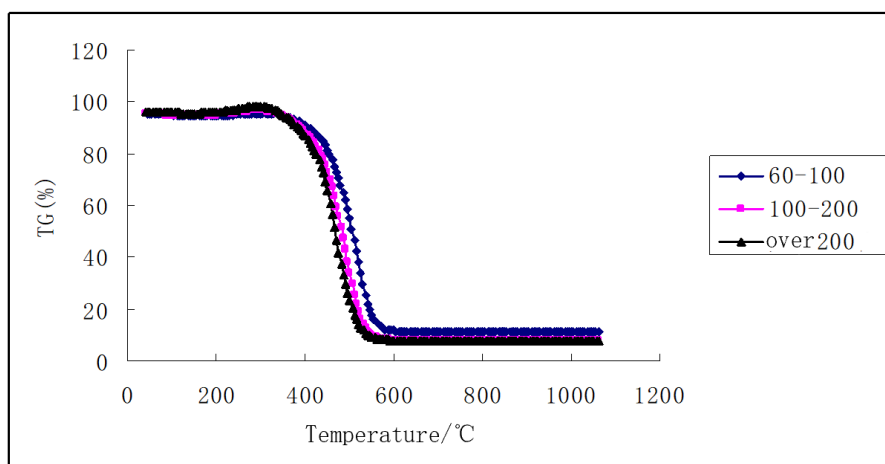


**Fig.3.5(a) Influence of different particle size on coal TG curve**

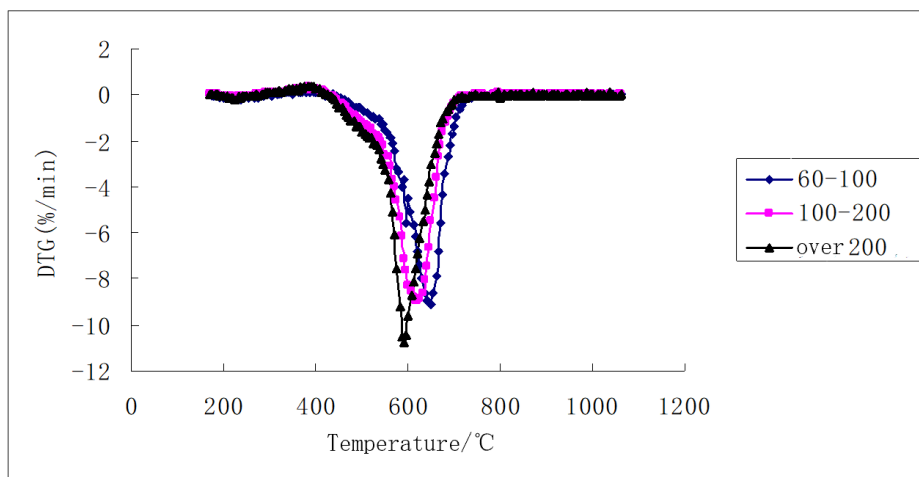


**Fig.3.5(b) Influence of different particle size on coal DTG curve**

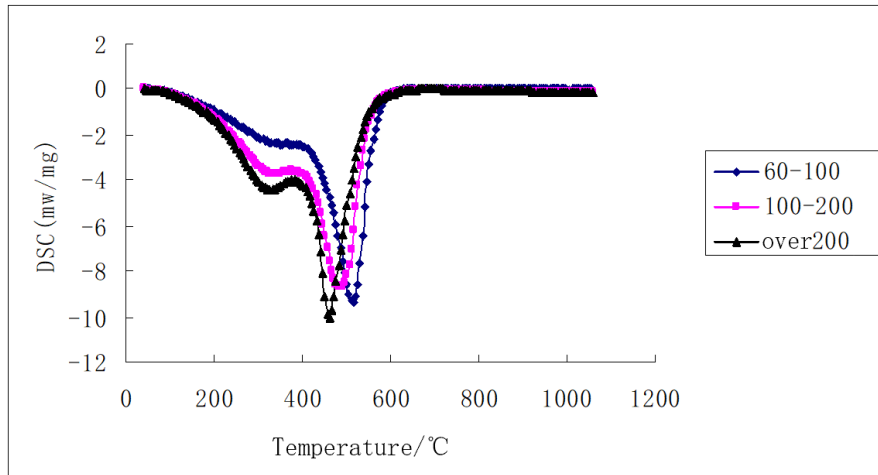


Fig.3.5(c) Influence of different particle size on coal DCS curve

### 3.5 Analysis of coal characteristic temperature points and reaction kinetic parameters

#### 3.5.1 Calculation of reaction kinetic parameters for coal

In the experiment, the carbon gasification reaction is a gas-solid reaction and the carbon conversion rate  $\alpha$  obtained during the gasification of the carbon powder is calculated by the formula (Wu et al. 2011):

$$\alpha = \frac{m_0 - m}{m_0 - m_\infty} = \frac{\Delta m}{\Delta m_\infty} \tag{2.38}$$

Where:  $m_0$  is the starting mass, kg;  $m$  is the mass at  $T(t)$ , kg;  $m_\infty$  is the final mass, kg;  $\Delta m$  is the mass loss at  $T(t)$ , kg;  $\Delta m_\infty$  is the maximum mass loss, kg.

The reaction mechanism of gas-solid multiphase reactions is very complex and the relationship between the gasification reaction rate and the conversion rate can usually be expressed using equation:

$$\frac{d\alpha}{dt} = Kf(\alpha)f(P_{O_2}) \tag{2.39}$$



where  $f(\alpha) = (1-\alpha)^n$ ,  $f(P_{O_2})$  is a function related to the partial pressure of oxygen, which is essentially constant during combustion,  $f(P_{O_2})$  is a constant,  $t$  is the reaction time,  $s$ ;  $n$  is the number of reaction stages; and  $K$  is the rate constant. According to the Arrhenius formula:

$$K = A \exp(-E/R_0T) \quad 2.40$$

where  $A$  is the pre-factor,  $E$  is the activation energy,  $R_0$  is the gas reaction constant,  $8.314 \text{ J/mol}$ , and  $T$  is the  $K$  temperature. At a constant rate of warming,  $\beta$  ( $\beta = dT/dt$ ), brought in and transformed by mathematical integration, gives

$$n \neq 1$$

$$\ln \left| \frac{1 - (1-a)^{(1-n)}}{T^2(1-n)} \right| = \ln \left[ \frac{AR_0}{\beta E} \left( 1 - \frac{2R_0T}{E} \right) \right] - \frac{E}{R_0T} \quad 2.41$$

$$n = 1$$

$$\ln \left| \frac{-\ln(1-a)}{T^2} \right| = \ln \left[ \frac{AR_0}{\beta E} \left( 1 - \frac{2R_0T}{E} \right) \right] - \frac{E}{R_0T} \quad 2.42$$

Since the first term at the left end of equations 2.41, 2.42 is approximated

as a constant for the general reaction zone and for most values of  $E \frac{E}{R_0T} \gg 1$ ,

i.e.  $(1 - \frac{2R_0T}{E}) \approx 1$ . Thus, at the reaction level  $n \neq 1$ , using equation 2.41 to graph

$1/T$  from  $\ln \left| \frac{1 - (1-a)^{(1-n)}}{T^2(1-n)} \right|$  gives a straight line with slope  $-E/R_0$ , from which the activation energy is obtained, and then the intercept of the straight line is used to find the frequency factor. Similarly, when  $n = 1$  is used, equation 2.42 is used to find the activation energy  $E$  and the finger front factor  $A$ .

Domestic and international studies have shown that the carbon gasification reaction has a number of stages  $n=1$ . Combining its activation energy  $E$  and frequency factor  $A$  obtained by graphing and linear regression of equation 2.42, the fitted curves for the kinetic parameters of the Tingnan coal sample are

shown in Figure 3.7, relative to the other three coal mines as shown in Figures 3.6 to 3.9.

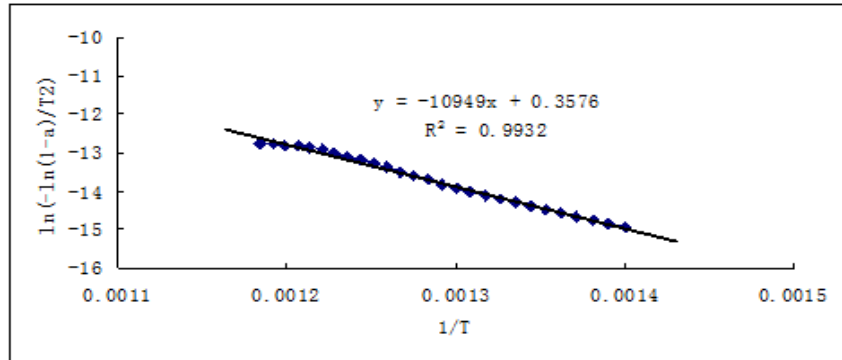


Fig.3.6 Fitted curve of Xingtiao coal sample

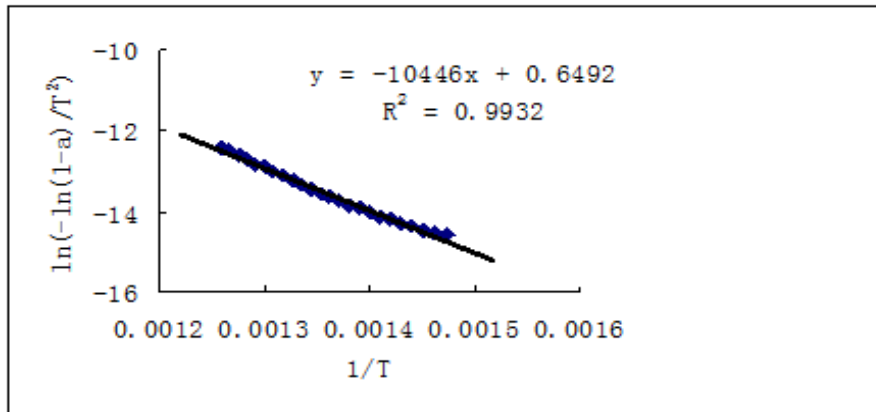


Fig.3.7 Fitted curve of the Tingnan coal sample

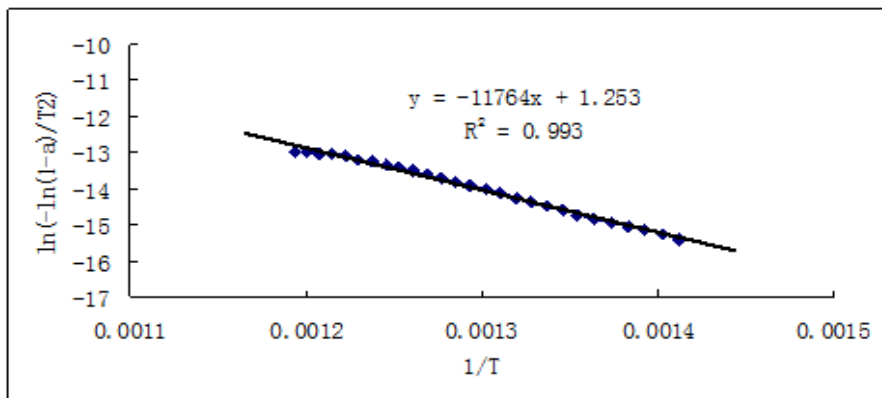
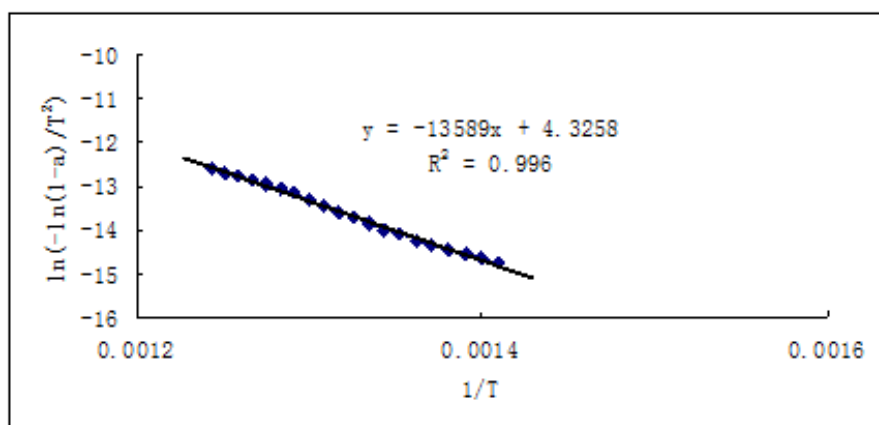


Fig.3.8 Fitted curve of coal sample from Xing County



**Fig.3.9 Fitted curve of Tangshan coal sample**

**Table 3.1 Coastsredfern method for solving kinetic parameters of 4 coal samples**

Parameters	Coal samples			
	Xingtao	Tingnan	Xing County	Tangshan
A ( $10^5$ )	2.0	1.57	4.12	102.77
E (KJ/mol)	86.85	91.03	97.8	112.98
R	0.997	0.997	0.997	0.998

### 3.5.2 Relationships between characteristic coal temperature points, reaction kinetic parameters and volatiles and elements

#### 1) Qualitative analysis

The finger front factor A and activation energy E of the coal were plotted separately to derive the relationship between the reaction kinetic parameters of the coal, the characteristic temperature point and the volatile content of the coal, as shown in Figure 3.10, where the trend of the temperature values of  $T_1 - T_4$  is not obvious enough (Xie et al. 2010).

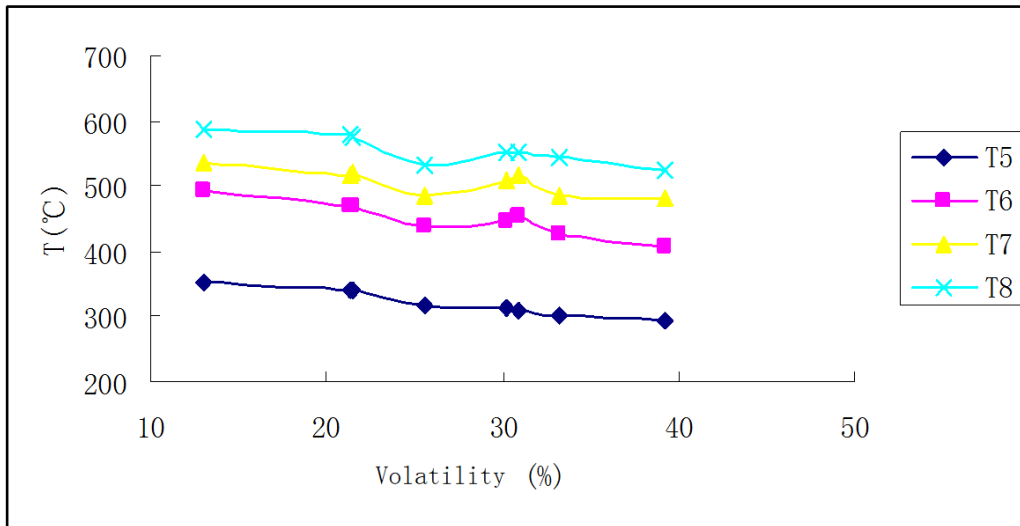


Figure 3.10 (a) Coal reaction kinetic parameters as a function of volatiles

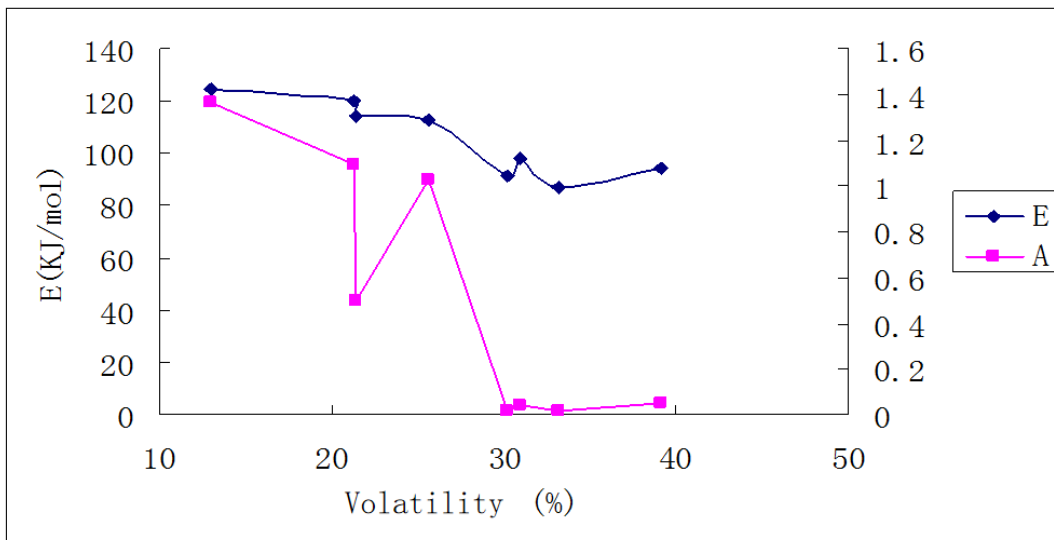


Figure 3.10 (b) Coal reaction kinetic parameters versus volatiles

2) Quantitative analysis

(1) Relationship between characteristic temperature and elemental analysis

① First characteristic point (correlation 0.98)

$$T_1 = 5.15N^{0.807}C^{0.791}S^{0.0519}H^{-0.5348}O^{0.0483}$$

② Second characteristic point (correlation 0.94)

$$T_2 = 10537.2N^{1.659}C^{-0.802}S^{-0.148}H^{-0.751}O^{-0.089}$$

(iii) Third characteristic point (correlation 0.91)

$$T_3 = 262.43N^{1.265}C^{0.089}S^{-0.04998}H^{-0.7}O^{-0.0609}$$

④ Fourth characteristic point (correlation 0.97)

$$T_4 = 685.37N^{-0.1707}C^{-0.1097}S^{0.039}H^{-0.039}O^{-0.1488}$$

⑤ Fifth characteristic point (correlation 0.98)

$$T_5 = 212.9N^{-0.538}C^{0.139}S^{-0.00832}H^{0.171}O^{-0.141}$$

(vi) Sixth characteristic point (correlation 0.99)

$$T_6 = 80.66N^{-0.502}C^{0.506}S^{0.009}H^{-0.169}O^{-0.048}$$

(vii) Seventh characteristic point (correlation 0.99)

$$T_7 = 60.11N^{-0.526}C^{0.583}S^{0.026}H^{-0.178}O^{8.306}$$

(viii) Eighth characteristic point (correlation 0.96)

$$T_8 = 96.34N^{-0.451}C^{0.461}S^{0.0126}H^{-0.043}O^{-0.029}$$

(2) Relationship between industrial parameters and characteristic points (moisture, HFF volatiles, HF ash, GDT fixed carbon, Sulphur)

① First feature point (correlation 0.97)

$$T_1 = 9457.42SF^{-0.0885}HFF^{-0.374}HF^{-0.269}GDT^{-0.659}S^{0.0468}$$

② Second characteristic point (correlation 0.97)

$$T_2 = 8102339262.2851SF^{0.0244}HFF^{-1.59}HF^{-0.446}GDT^{-2.88}S^{0.0809}$$

(iii) Third characteristic point (correlation 0.91)

$$T_3 = 386007614.01SF^{-0.12}HFF^{-1.186}HF^{-0.481}GDT^{-2.362}S^{0.028}$$

④ Fourth characteristic point (correlation 0.97)

$$T_4 = 328.26SF^{-0.047}HFF^{-0.105}HF^{0.00934}GDT^{0.0523}S^{0.0252}$$

⑤ Fifth characteristic point (correlation 0.99)

$$T_5 = 2.89SF^{-0.0202}HFF^{0.249}HF^{0.136}GDT^{0.889}S^{-0.045}$$

(vi) Sixth characteristic point (correlation 0.98)

$$T_6 = 6.792SF^{-0.0173}HFF^{0.234}HF^{0.0947}GDT^{0.796}S^{-0.0595}$$

(vii) Seventh characteristic point (correlation 0.96)

$$T_7 = 11.267SF^{0.0116} HFF^{0.209} HF^{0.0886} GDT^{0.718} S^{-0.0359}$$

(viii) Eighth characteristic point (correlation 0.95)

$$T_8 = 7.285SF^{-0.0055} HFF^{0.266} HF^{0.1024} GDT^{0.798} S^{-0.0404}$$

(3) Maximum burning rate versus element (correlation 0.94)

$$V_{\max} = 22.404N^{-0.0478} C^{-0.733} S^{-0.2598} H^{2.0617} O^{-0.29987}$$

(4) Activation energy in relation to elements and coal quality

① Activation energy versus elements (correlation 0.93)

$$E = 4.76 \times 10^9 N^{1.29} C^{-3.99} S^{-0.12} H^{1.73} O^{-1.95}$$

② Relationship between activation energy and coal quality (correlation 0.99)

$$E = 7.36 \times 10^5 SF^{-7} HFF^{2.83} HF^{-1.17} GDT^{-3.15} S^{-4.16}$$

(5) Relationship between pre-exponential factors and elements and coal quality

① Relationship between pre-exponential factors and elements (correlation 0.99)

$$A = 3696N^{0.15} C^{-0.74} S^{0.002} H^{0.19} O^{-0.31}$$

② Relationship between pre-index factor and coal quality (correlation 0.99)

$$A = 2859SF^{-0.09} HFF^{-0.39} HF^{-0.065} GDT^{-0.45} S^{0.039}$$

From Figure 3.5, the above formula shows that: ① As the volatile content increases, each characteristic temperature, gradually becomes smaller, which means that the coal combines with the oxygen in the air to increase the weight of the coal to the maximum point of the temperature value, the ignition point temperature, the maximum weight loss temperature and the combustion temperature are all pushed forward. It can be deduced from this that the more volatile the coal, the easier it is to ignite and the sooner it burns out. However, the volatile content does not vary linearly with the characteristic temperature

point, which means that volatile content is not the only factor affecting the characteristic temperature, but there may be other influences (sulphur content, hydrogen content, etc.). ② As the volatile content increases, the activation energy  $E$  of the coal tends to decrease. This is due to the fact that the more volatiles there are, the more the combustion of volatiles can ignite the coal particles; in addition, the precipitation of volatiles changes the phase structure of the coke, making the remaining coke porous, and the more volatiles there are, the larger the specific surface area of the remaining coke, the larger the contact area with air, and the easier it is to ignite, so the minimum energy required for the coal combustion reaction, i.e. the activation energy  $E$  value, is also smaller. (iii) As the volatile content increases, the prefactor  $A$  also tends to decrease. This is due to the fact that the more volatile the coal, the lower the activation energy  $E$ . When the volatile content is greater than 30%, the change in this is relatively smooth.

---

### **3.5.3 Experimental conclusions**

---

(1) The higher the volatile content, the lower the value of the characteristic temperature of combustion of the coal and the smaller the value of the thermodynamic parameters (activation energy, pre-exponential factor). This means that the easier the coal is to ignite and the higher the risk of spontaneous combustion of the coal.

(2) The characteristic temperature values, thermodynamic parameters and volatile matter of coal are not linearly related, and may be related to other factors. Therefore, it is necessary to study the factors affecting the natural tendency of coal based on the industrial analysis of coal, to establish a system for evaluating the risk of spontaneous combustion of coal based on the industrial parameters of coal, and to achieve a rapid analysis of the risk of spontaneous combustion of coal.

## 3.6 Fourier transform infrared spectroscopy of coal

### 3.6.1 Characteristic gas analysis for thermal decomposition of coal

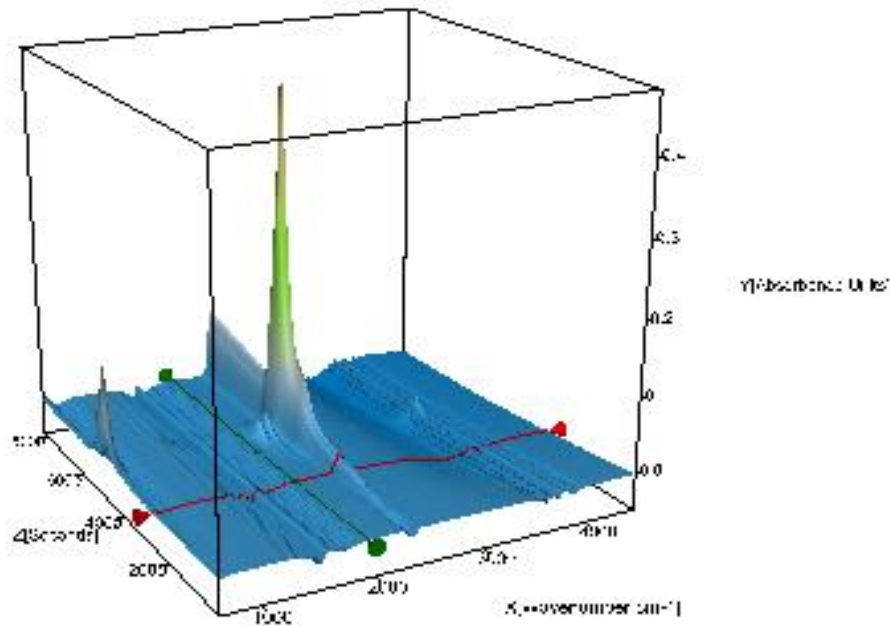


**Fig.3.11 (a) 3D diagram of the precipitation of gases from the thermal decomposition of coal**

In the process of thermal decomposition of coal, due to its coal quality, the types and concentrations of the gases produced are different, the main gas components are CO, CO<sub>2</sub>, CH<sub>4</sub>, SO<sub>2</sub> etc. Figure 3.11 (a) and (b) shows the thermal decomposition of coal with a heating rate of 10°C/min, oxygen concentration of 21% and particle size <0.178mm (Ju et al.2005).



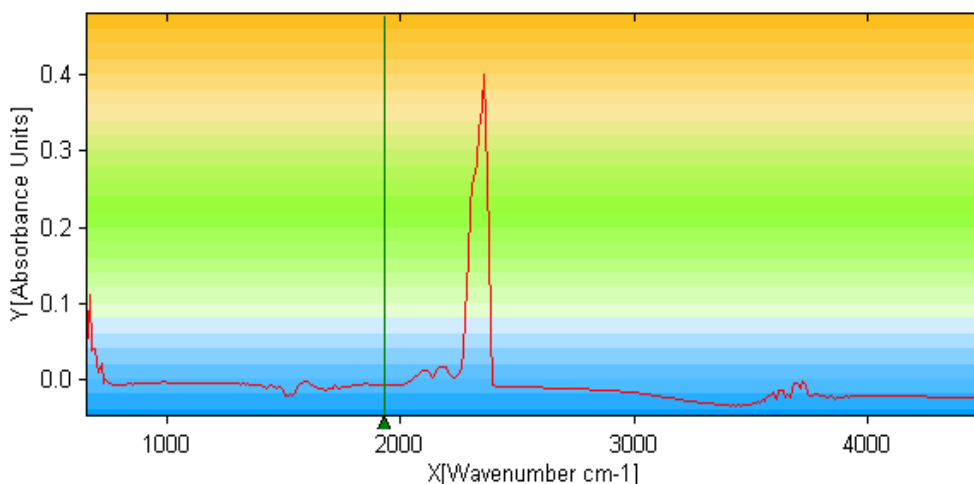


**Fig.3.11 (b) Graph of maximum absorption intensity of gases precipitated by thermal decomposition of coal**

From FTIR detection, it is known that the gases produced during the combustion of fixed carbon by adding oxygen after the precipitation of volatile matter from coal are CO<sub>2</sub> and a small amount of H<sub>2</sub>O. The other gases that cause pollution to the environment are basically released during the pyrolysis process. From the absorption peaks of the FTIR spectrum, we know that the absorption peaks of CO<sub>2</sub> range from 2650 - 2200cm<sup>-1</sup> and 850 - 400cm<sup>-1</sup> , the absorption peaks of H<sub>2</sub>O range from 1750 - 1500cm<sup>-1</sup> , the absorption peaks of CH<sub>4</sub> range from 3100 -2800cm<sup>-1</sup> and 1400 - 1100cm<sup>-1</sup> , the absorption peaks of CO range from 2200 -1900cm<sup>-1</sup>, and C<sub>2</sub>H<sub>4</sub> in the range of 3000 - 3100cm<sup>-1</sup>. Figure 3.12 shows the gas precipitation peaks at the characteristic temperature points T<sub>2</sub> , T<sub>4</sub> and T<sub>5</sub> for the Tingnan coal sample.

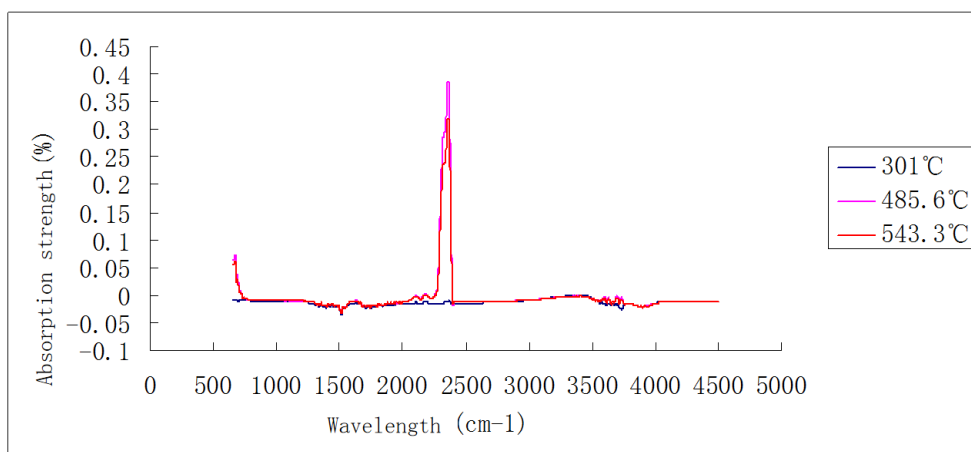


**Fig.3.12 Gas precipitation at characteristic temperature points**

Figure 3.12 Absorption peaks for CO<sub>2</sub> at 2650 - 2200cm<sup>-1</sup> Absorption peaks for H<sub>2</sub>O at 1750 - 1500cm<sup>-1</sup>, for CH<sub>4</sub> at 1400 - 1100cm<sup>-1</sup> and for CO at 2200 - 1900cm<sup>-1</sup>. However, the absorption intensities of their respective fronts differ, being much smaller at the T<sub>2</sub> temperature point than at the maximum burning rate point and the termination point temperature. This is because the strength of the absorption peak is related to the pyrolysis temperature of the coal molecules. The absorption intensities also vary between coal samples, due to the fact that the intensity of the absorption peaks is also related to the structure of the coal macromolecular network.

### 3.6.2 Analysis of the functional groups of coal

To test the functional groups of coal, KBr powder and coal samples are mixed and ground at a ratio of 180:1 (approximately 0.0995 g for KBr and 0.0005g for coal), pressurised (10 MP) on a tablet press, pressurised for 1 min, unpressurised and the film removed to obtain a 0.1 mm thick circular transparent sheet, which is placed in an IR spectrometer sample for test scanning. The wave number range was from 400 to 4000cm<sup>-1</sup> with a resolution of 4.0cm<sup>-1</sup>, and the number of scans was accumulated to 32 for 1 min. The characteristic values of the main functional group spectral peaks of the experimental coal samples are shown in Table 3.2, and the characteristic absorption peaks of the Tingnan Mine coal samples are shown in Figure 3.13.

**Table 3.2 Table of main characteristics of coal absorption peaks**

Spectral peak number	Spectral peak position/cm <sup>-1</sup>	Functional groups	Wavelength/ $\mu$ m	Attribution
1	1264-1255	Ar-CO	7.88	Ether-oxygen bonds
2	1379-1373	-CH <sub>3</sub>	7.52	Methyl shear vibration
3	1706-1705	C=O	5.88	Aromatic ketone carbonyl group
4	2858-2847	-CH <sub>2</sub>	3.52	Methylene-symmetric telescopic vibrations
5	753-743	-CH <sub>2</sub>	13.51	Methylene plane vibration

Spectral peak number	Spectral peak position/cm <sup>-1</sup>	Functional groups	Wavelength/ $\mu\text{m}$	Attribution
6	1449-1439	-CH <sub>2</sub>	6.99	Methylene shear vibration
7	2922-2918	-CH <sub>2</sub> -CH <sub>3</sub>	3.43	Methylene, methylene asymmetric stretching vibrations
8	1604-1599	C=C	6.25	C=C stretching vibrations in aromatic rings
9	3697-3684 3624-3613	-OH	2.74	Alcohols, hydroxy, phenols
10	1736-1722	$\begin{array}{c} \text{O} \\ \parallel \\ -\text{C}-\text{OH} \end{array}$	5.83	Ketones, aldehydes, esters of carbonyl groups
11	1026-912		10.95	Minerals
12	819-799		12.07	Substituted benzenes

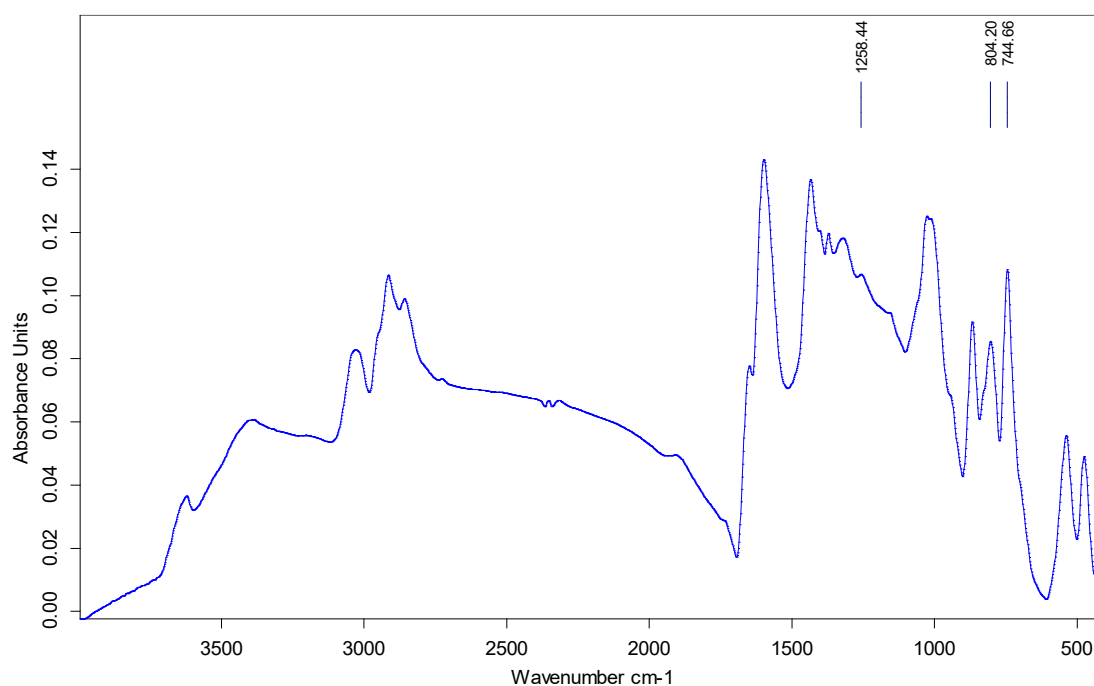


**Fig.3.13 Spectroscopy of the functional group of Tingnan**

(1) By analysing the precipitated gases at the characteristic temperature points when coal is thermally decomposed, the laws and types of gases precipitated by thermal decomposition of coal can be known, providing a theoretical basis for the prevention and control of spontaneous combustion of coal.

(2) The analysis of the characteristic peaks of the functional groups of the coal will provide information on the content and type of functional groups within

the coal, in preparation for further analysis of the ability of the coal to oxidise and spontaneously combust.

---

## **4 Analysis of index gases**

---

According to the coal-oxygen composite theory, the coal spontaneous combustion process can be divided into three stages according to the characteristics of temperature, physical and chemical reactions, namely the incubation period, the self-heating period and the combustion period. The regular correspondence between the concentration of marker gas and temperature and the three stages of coal spontaneous combustion process is the theoretical basis for coal spontaneous combustion early warning. However, under the effect of wind flow dilution, nitrogen injection and gas gushing, CO and its indicators usually change, which may lead to misjudgement of coal spontaneous combustion and fire area by decision makers. Therefore, it is crucial to consider the effect of wind flow dilution, nitrogen injection and gas gushing on CO and its indicators, eliminate the influencing factors and select suitable indicators for coal spontaneous combustion early warning. In this chapter, the trends of CO and its indicators under the effects of wind flow dilution and nitrogen injection will be investigated by means of theoretical derivation, in order to grasp the relevant laws and apply them to the early warning of coal spontaneous combustion (Kou et al. 2012).

---

### **4.1 Analytical study of CO and its indicators**

---

CO appears early in the process of oxidative spontaneous combustion of coal, is produced in larger quantities and its concentration increases at a faster rate, and there is an obvious correspondence between its concentration and the temperature of the coal body.

However, CO is also readily adsorbed by coke and carbon black, creating the illusion that the fire is extinguished. In addition it can be decomposed by some

fungi or adsorbed by wet coal, and this decomposition and adsorption can be significant for carbon monoxide produced by fires. So there exist some composite indicators that can be used as an aid to prediction, the main ones being the carbon oxide ratio, calculated as shown in equation 4.1.

(2) Carbon oxide ratio  $R_{CO}$

The carbon oxide ratio  $R_{CO}$  represents the ratio between the CO concentration and the CO<sub>2</sub> concentration. The CO ratio is used to indicate the development of a fire, where it increases in the early stages of the fire and remains a constant during the full combustion stage. In the absence of non-combustion generated carbon oxides, the increase in CO<sub>2</sub> concentration with temperature follows a similar trend to the increase in CO concentration with temperature, and the carbon oxide ratio is the only indicator of all judgement indicators where the ratio is not affected by wind flow, CH<sub>4</sub> gush and injection of inert gas, and is calculated as shown in equation 4.1.

$$R_{CO} = \frac{CO}{CO_2} \quad 4.1$$

The microscopic essence of coal spontaneous combustion is mainly a variety of different structures in the coal molecules, at a particular temperature, respectively, physical-chemical adsorption and chemical reactions with oxygen, and its macroscopic manifestation is the change of gas concentration produced at a specific temperature, the temperature is the characteristic temperature of the coal spontaneous combustion process. Among them, the critical temperature is the turning point of coal from the low temperature oxidation stage to the rapid oxidation stage, coal oxygen compounding begins to strengthen, the macroscopic performance is a sharp increase in CO concentration, according to the sign gas analysis method, when the CO concentration curve appears inflection point, it means that the characteristic temperature reaches the critical temperature; after that, the gas concentration

rises sharply, the exothermic intensity of coal body increases, the oxygen consumption rate rises faster, when the coal temperature reaches the dry cracking temperature, coal molecules oxidation reaction occurs to produce  $C_2H_4$  gas and a second sharp increase in CO concentration occurs. Therefore, in the marker gas growth rate graph and the marker gas relative growth rate graph, the first peak in the CO growth rate curve occurs when the oxidation reaches the critical temperature, and the second peak in the CO growth rate curve occurs when the dry cracking temperature is reached, which can be used to determine the characteristic temperature point.

---

## **4.2 Analysis of the effect of wind flow dilution on CO and its indicators**

---

Due to the presence of primary CO from the coal remnants, as well as the low temperature oxidation of the coal and the spontaneous combustion of the coal, a certain amount of CO will always be present in the mined area, and due to air leakage, the CO from the mined area will be transported to the working face and the upper corner, thus affecting the CO concentration in the upper corner. This is the key to using grey correlation for early warning (Yu. 2014).

In order to explore the variation of CO related indicators in the mining area under the effect of wind flow dilution, this section starts from the upper corner and samples are taken along the way in the direction perpendicular to the working face to analyse the variation of CO concentration, while the variation of CO index  $I_{CO}$  and carbon oxide ratio  $R_{CO}$  are processed. If there is air leakage from the extraction area to the sampling point, the CO concentration will change; if there is air leakage from the sampling point to the outside of the extraction area, the CO concentration,  $I_{CO}$  and  $R_{CO}$  will not change. Therefore, the key of this section is to study the variation of CO concentration,  $I_{CO}$  and  $R_{CO}$  in the case of air leakage from the extraction area to the sampling point, and to obtain the theoretical law of CO transport under the effect of wind flow dilution. Based

on the theory, a simple model of the mined area with air leakage channels was constructed, as shown in Figure 4.1.

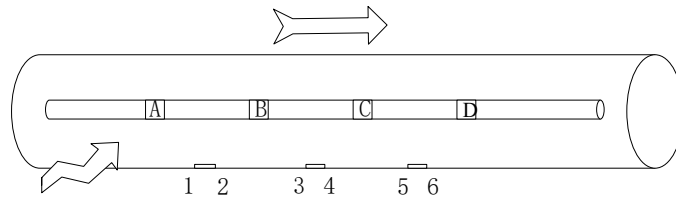


**Fig.4.1 Schematic diagram of the air leakage channel in the mining area**

Figure 4.1 shows a leaky passage in a mining area, A-D are the sampling points in the leaky passage, the direction of wind flow in the leaky passage is A to D (as shown by the arrow above), 1~2, 3~4, 5~6 indicate 3 leaky sections, the direction of air leakage is towards the leaky passage, at the same time, each sampling point is at a certain distance from the beginning and end of the respective adjacent leaky section (Luo et al. 2021).

Assume that the air leakage in each leakage section is  $\Delta Q$ , the leakage is fresh air flow, where the O concentration is  $C_{O_2} = 20.93\%$ , the CO concentration is  $C_{CO_2} = 0.03\%$  and the N<sub>2</sub> concentration is  $C_{N_2} = 79.04\%$  (the content of rare gases and the content of nitrogen are not affected by the external environment, so 0.97% of rare gases are incorporated into N<sub>2</sub> to do a uniform treatment to simplify the model). The air flow through point A is  $Q$ , where the CO concentration is  $C_{CO}^A$  (subscript indicates the gas type and superscript indicates the sampling point), the oxygen concentration is  $C_{O_2}^A$ , the CO<sub>2</sub> concentration is  $C_{CO_2}^A$  and the N<sub>2</sub> concentration is  $C_{N_2}^A$ .

Taking sampling points A and B as an example, the following relationship exists according to the law of conservation of mass.

$$\begin{aligned}
 Q_A C_{CO}^A &= (Q_A + \Delta Q_{12}) C_{CO}^B \\
 Q_A C_{CO_2}^A + \Delta Q_{12} C_{CO_2} &= (Q_A + \Delta Q_{12}) C_{CO_2}^B \\
 Q_A C_{O_2}^A + \Delta Q_{12} C_{O_2} &= (Q_A + \Delta Q_{12}) C_{O_2}^B \\
 Q_A C_{N_2}^A + \Delta Q_{12} C_{N_2} &= (Q_A + \Delta Q_{12}) C_{N_2}^B
 \end{aligned}
 \tag{4.2}$$

The concentration of each gas at sampling point B can thus be expressed as

$$\begin{aligned}
 C_{CO}^B &= \frac{Q_A C_{CO}^A}{Q_A + \Delta Q_{12}} \\
 C_{CO_2}^B &= \frac{Q_A C_{CO_2}^A + \Delta Q_{12} C_{CO_2}}{Q_A + \Delta Q_{12}} \\
 C_{O_2}^B &= \frac{Q_A C_{O_2}^A + \Delta Q_{12} C_{O_2}}{Q_A + \Delta Q_{12}} \\
 C_{N_2}^B &= \frac{Q_A C_{N_2}^A + \Delta Q_{12} C_{N_2}}{Q_A + \Delta Q_{12}}
 \end{aligned}
 \tag{4.3}$$

The ratios of carbon oxides at points A and B are

$$\begin{aligned}
 R_{CO}^A &= \frac{C_{CO}^A}{C_{CO_2}^A} \\
 R_{CO}^B &= \frac{C_{CO}^B}{C_{CO_2}^B}
 \end{aligned}
 \tag{4.4}$$

Substituting equation 4.6 into 4.7, we get

$$\begin{aligned}
 \Delta Q_{12} &= \frac{Q_A (C_{CO}^A - C_{CO}^B)}{C_{CO}^B} \\
 R_{CO}^B &= \frac{C_{CO}^B}{C_{CO_2}^B} = \frac{Q_A C_{CO}^A}{Q_A C_{CO_2}^A + \Delta Q_{12} C_{CO_2}}
 \end{aligned}
 \tag{4.5}$$

As can be seen from equation 4.8, the actual meaning of the denominator in the derivation formula for the carbon oxide ratio at point B is to indicate the absolute content of CO<sub>2</sub>, while the numerator indicates the absolute content of CO. In the absence of coal spontaneous combustion and fire in the mining area, CO is basically not produced, so the absolute content of CO in the mining area is kept constant; the absolute content of CO<sub>2</sub> in the air leakage is 0.03%, which



changes very little under the influence of non-fire factors and can be regarded as basically kept constant, so there is

$$R_{CO}^B \approx R_{CO}^A \quad 4.6$$

The carbon oxide ratio at point B is therefore largely unaffected by the fresh air flow.

The carbon monoxide index at point B is

$$I_{CO}^B = \frac{C_{CO}^B}{0.265C_{N_2}^B - C_{O_2}^B} \quad 4.7$$

Substituting equation 4.6 into equation 4.10 yields

$$I_{CO}^B = \frac{Q_A C_{CO}^A}{0.265(Q_A C_{N_2}^A + \Delta Q_{12} C_{N_2}) - (Q_A C_{O_2}^A + \Delta Q_{12} C_{O_2})} \quad 4.8$$

In the formula for the derivation of the CO index from equation 4.11, the numerator represents the absolute amount of CO and the denominator represents the mathematical operation between the absolute amount of N<sub>2</sub> and the absolute amount of O<sub>2</sub>. Similarly, the carbon monoxide index and carbon oxide ratio at point C are

$$I_{CO}^C = \frac{Q_A C_{CO}^A}{0.265(Q_A C_{N_2}^A + \Delta Q_{12} C_{N_2} + \Delta Q_{34} C_{N_2}) - (Q_A C_{O_2}^A + \Delta Q_{12} C_{O_2} + \Delta Q_{34} C_{O_2})} \quad 4.9$$

$$R_{CO}^C = \frac{Q_A C_{CO}^A}{Q_A C_{CO_2}^A + \Delta Q_{12} C_{CO_2} + \Delta Q_{34} C_{CO_2}}$$

Comparing equations 4.9 and 4.11 and analysing them in conjunction with equation 4.12, the absolute CO content is calculated for both the numerator term of the CO index and the carbon oxide ratio, the denominator term of the CO index is the mathematical operation of the absolute content of N<sub>2</sub> and O<sub>2</sub>, and the denominator term of the carbon oxide ratio is the absolute content of CO<sub>2</sub>. In the fresh air flow, the content of N<sub>2</sub> and O<sub>2</sub> reaches 99.7%, while the content of CO<sub>2</sub> is only 0.03%. In the case of a small amount of air leakage, the fresh air flow has a small effect on the CO index value, but in the case of a large

amount of air leakage, the fresh air flow has a more obvious effect on the absolute content of  $N_2$  and  $O_2$  in the leakage channel, and the change in the absolute content of  $N_2$  and  $O_2$  affects the change in the CO index value; on the contrary, the carbon oxide ratio, the effect of air leakage on the absolute content of  $CO_2$  is small and much smaller than the effect of air leakage on the absolute content of  $N_2$  and  $O_2$ , irrespective of the amount of air leakage, so it can be concluded that the carbon oxide ratio is largely unaffected by the dilution effect of the air flow (Xia et al. 2016).

### 4.3 Analysis of the effect of nitrogen injection on CO and its indicators

In considering the effect on CO and indicators when injecting nitrogen into the extraction area, the air leakage channel schematic of Figure 4.1 is still used, at this time, the air leakage volume of each leakage section  $\Delta Q$  is all  $N_2$ , and the air flow rate through point A is  $Q$ , where the CO concentration is  $C_{CO}^A$  (the same below, the subscript indicates the gas type and the superscript indicates the sampling point), the oxygen concentration is  $C_{O_2}^A$ , the  $CO_2$  concentration is  $C_{CO_2}^A$ , and the  $N_2$  concentration is  $C_{N_2}^A$ . Using sampling points A and B as examples, the following relationships exist according to the law of conservation of mass.

$$\begin{aligned}
 Q_A C_{CO}^A &= (Q_A + \Delta Q_{12}) C_{CO}^B \\
 Q_A C_{CO_2}^A &= (Q_A + \Delta Q_{12}) C_{CO_2}^B \\
 Q_A C_{O_2}^A &= (Q_A + \Delta Q_{12}) C_{O_2}^B \\
 Q_A C_{N_2}^A + \Delta Q_{12} C_{N_2} &= (Q_A + \Delta Q_{12}) C_{N_2}^B
 \end{aligned}
 \tag{4.10}$$

The concentration of each gas at sampling point B can thus be expressed as

$$\begin{aligned}
 C_{CO}^B &= \frac{Q_A C_{CO}^A}{Q_A + \Delta Q_{12}} \\
 C_{CO_2}^B &= \frac{Q_A C_{CO_2}^A}{Q_A + \Delta Q_{12}} \\
 C_{O_2}^B &= \frac{Q_A C_{O_2}^A}{Q_A + \Delta Q_{12}} \\
 C_{N_2}^B &= \frac{Q_A C_{N_2}^A + \Delta Q_{12} C_{N_2}}{Q_A + \Delta Q_{12}}
 \end{aligned}
 \tag{4.11}$$

The ratio of carbon oxides at point B can be deduced to be

$$R_{CO}^B = \frac{C_{CO}^B}{C_{CO_2}^B} = \frac{C_{CO}^A}{C_{CO_2}^A} = R_{CO}^A
 \tag{4.12}$$

Equation 4.15 shows that the carbon oxide ratio at point B is not affected by the nitrogen injection.

For the CO index at point B, it can be deduced that

$$I_{CO}^B = \frac{C_{CO}^B}{0.265 C_{N_2}^B - C_{O_2}^B} = \frac{Q_A C_{CO}^A}{0.265(Q_A C_{N_2}^A + \Delta Q_{12} C_{N_2}) - Q_A C_{O_2}^A}
 \tag{4.13}$$

The numerator represents the absolute content of CO and the denominator represents the mathematical operation of the absolute content of N<sub>2</sub> and O<sub>2</sub>. When a large amount of nitrogen is injected into the extraction area, the size of the denominator will be affected by the nitrogen, from to resulting in a change in the CO index. Similarly, the carbon monoxide index and carbon oxide ratio at point C is

$$\begin{aligned}
 I_{CO}^C &= \frac{Q_A C_{CO}^A}{0.265(Q_A C_{N_2}^A + \Delta Q_{12} C_{N_2} + \Delta Q_{34} C_{N_2}) - Q_A C_{O_2}^A} \\
 R_{CO}^C &= \frac{Q_A C_{CO}^A}{Q_A C_{CO_2}^A}
 \end{aligned}
 \tag{4.14}$$

Comparing equation 4.15 with equation 4.16 and analysing it in conjunction with equation 4.17, it is concluded that when nitrogen is injected into the extraction zone, the carbon oxide ratio will remain constant, while the carbon monoxide index will be affected and will vary.

## 4.4 Analysis of the effect of gas emergence on CO and its indicators

When gas gushing occurs in the mining area and affects the leaky air passage, the leaky air passage model in Figure 4.1 is used for the study, at this time, the leaky air volume of each leaky section  $\Delta Q$  is regarded as all CH<sub>4</sub>, and the air flow rate through point A is  $Q$ , where the CO concentration is  $C_{CO}^A$ , the oxygen concentration is  $C_{O_2}^A$ , the CO<sub>2</sub> concentration is  $C_{CO_2}^A$ , and the N<sub>2</sub> concentration is  $C_{N_2}^A$ . Using sampling points A and B as examples, the following relationships exist according to the law of conservation of mass.

$$\begin{aligned} Q_A C_{CO}^A &= (Q_A + \Delta Q_{12}) C_{CO}^B \\ Q_A C_{CO_2}^A &= (Q_A + \Delta Q_{12}) C_{CO_2}^B \\ Q_A C_{O_2}^A &= (Q_A + \Delta Q_{12}) C_{O_2}^B \\ Q_A C_{N_2}^A &= (Q_A + \Delta Q_{12}) C_{N_2}^B \end{aligned} \quad 4.15$$

The concentration of each gas at sampling point B can thus be expressed as

$$\begin{aligned} C_{CO}^B &= \frac{Q_A C_{CO}^A}{Q_A + \Delta Q_{12}} \\ C_{CO_2}^B &= \frac{Q_A C_{CO_2}^A}{Q_A + \Delta Q_{12}} \\ C_{O_2}^B &= \frac{Q_A C_{O_2}^A}{Q_A + \Delta Q_{12}} \\ C_{N_2}^B &= \frac{Q_A C_{N_2}^A}{Q_A + \Delta Q_{12}} \end{aligned} \quad 4.16$$

The ratio of carbon oxides at point B can be deduced to be

$$R_{CO}^B = \frac{C_{CO}^B}{C_{CO_2}^B} = \frac{C_{CO}^A}{C_{CO_2}^A} = R_{CO}^A \quad 4.17$$

From equation 4.20, it can be seen that the carbon oxide ratio at point B is unaffected by the gas gush.

For the CO index at point B, it can be deduced that

$$I_{CO}^B = \frac{C_{CO}^B}{0.265C_{N_2}^B - C_{O_2}^B} = \frac{Q_A C_{CO}^A}{0.265Q_A C_{N_2}^A - Q_A C_{O_2}^A} \quad 4.18$$

The numerator represents the absolute content of CO and the denominator represents the mathematical operation of the absolute content of N<sub>2</sub> and O<sub>2</sub>. When gas gushes out of the mining area, both the numerator and denominator are unaffected, therefore, the CO index is not affected by the gas gusher. Similarly, the carbon monoxide index and carbon oxide ratio at point C is

$$I_{CO}^C = \frac{Q_A C_{CO}^A}{0.265Q_A C_{N_2}^A - Q_A C_{O_2}^A} \quad 4.19$$

$$R_{CO}^C = \frac{Q_A C_{CO}^A}{Q_A C_{CO_2}^A}$$

Combining the analysis of Equation 4.17, Equation 4.18 and Equation 4.19, it is concluded that neither the carbon oxide ratio nor the carbon monoxide index are affected by changes in the gas gush in the extraction area.

In summary, the carbon oxide ratio is not influenced by fresh air flow, nitrogen injection and gas gush; while the carbon monoxide index is influenced by fresh air flow and nitrogen injection, not by gas gush. Therefore, considering that the mined area is affected by fresh air flow, nitrogen injection and gas gushing, it is more appropriate to use the carbon oxide ratio as an indicator of coal spontaneous combustion warning.

---

## 4.5 Determination of index gases from natural coal seam fires

---

### 4.5.1 Basis and content of determination

---

1) Basis of measurement

(1) AQ/T1019-2006 Method for the chromatographic analysis of coal seam natural ignition marker gases and index preference.

(2) GB482-1995 Method of taking coal samples from coal seams.

(3) GB474-1996 Method of preparing coal samples.

(4) Coal Mine Safety Regulations (2016 Edition).

(5) Contract for "Testing of Basic Parameters for Spontaneous Combustion of Coal in Tingnan Coal Mine" between Shaanxi Changwu Tingnan Coal Mine Limited Liability Company and Coal Science and Technology Research Institute Co.

---

#### **4.5.2 Principle of determination**

Natural coal ignition is due to the physical and chemical adsorption and chemical reactions that occur when coal comes into contact with oxygen to release heat, and when the heat released is greater than the heat given off, the coal temperature rises and leads to ignition. The natural coal ignition process can be divided into three different stages of development: slow oxidation, accelerated oxidation and violent oxidation, as shown in Figure 4.2. By simulating the spontaneous combustion process of coal oxidation at low temperatures, the concentrations of gases such as CO, CO<sub>2</sub>, CH<sub>4</sub>, etc. are measured during the warming process of coal samples, and the values and changes of characteristic parameters such as oxygen consumption rate are calculated, while the parameters such as critical temperature and dry cracking temperature of coal samples are analysed according to the experimental results, so as to identify and judge the occurrence of coal spontaneous combustion and its development degree.

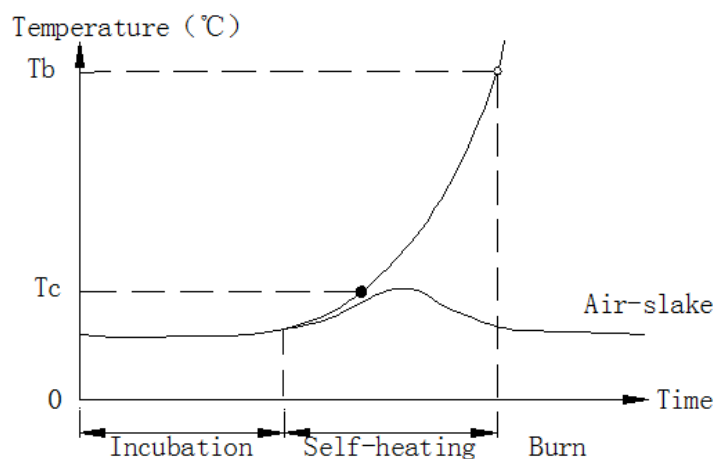


**Fig.4.2 Evolution of natural coal firing**

### 4.5.3 Test equipment

(1) Test system: dry air bottle, gas preheating copper tube, coal sample tank, thermostat, gas collection system, gas analysis system (gas chromatograph), data acquisition system. The details are shown in Figures 4.3.

- (2) Jaw Crusher
- (3) Sealed sample making machine
- (4) Sieving machines
- (5) Scales



**(a) Programmed temperature oven (b) GC-4008B gas chromatograph (c) Gas chromatograph analysis software**

**Fig.4.3 Coal natural ignition marker gas preference test system**

#### 4.5.4 Experimental steps

---

(1) Preparation of coal samples in accordance with GB 474-2008, while meeting the following requirements (Wang.2006):

① Use the stacked cone quartile method to divide to 500g~600g for the preparation of analytical coal samples, the rest of the coal samples are sealed and stored under seal for enquiry.

② After crushing the coal samples, the samples are separated by particle size using a vibrating sieve machine according to the test requirements.

(iii) Store the measured coal sample in a wide-mouth bottle in a sealed container and complete the determination of the relevant parameters within 7 days.

④ Original coal samples and analytical coal sample identification reports on file.

(2) Instrument inspection and sample loading

① Check the airtightness of the apparatus.

② Check the operating status of temperature sensors and data acquisition systems and debug any problems.

③ Commissioning of the gas chromatograph.

④ After making sure that the airtightness is good and that all relevant instruments are functioning properly, load the coal sample to be measured.

⑤ Check the gas tightness of the instrument again after loading the sample.

(3) Calibration of the gas chromatograph: The difference between the analytical results of two consecutive standard gases is within  $\pm 0.02\%$ .

(4) Dry air is introduced into the coal sample tank at a steady flow rate of 60 ml/min, at which point the system is started and the tank is heated with an edited program (or warmed up according to the coal temperature), and gas samples are collected at 10°C intervals starting at 30°C. At this time, data such as time ambient temperature is recorded, and the gas samples are analysed through the chromatograph until a predetermined temperature is reached.



(5) Recording and processing of data.

(6) Notes

① The top of the temperature sensor is placed in the geometric centre of the coal sample.

② The injection of gas into the chromatograph requires strict time control.

(iii) Keep an eye on the temperature of the coal sample during the warming process to avoid forgetting to take a gas sample.

④ Care should be taken during the collection of gas samples to ensure that no indoor gases are collected and that the samples are pure.

⑤ Due to the programmed temperature rise during the experiment, the temperature of the thermostat is high, at this time you need to pay attention to the experimental process must not open the thermostat at will.

(6) Pay attention to the ventilation of the room and the collection of exhaust fumes.

---

### **4.5.5 Gas samples Testing**

---

The GC-4000A manufactured by East-West Electronics was used to analyse the gas samples produced during the warming process of the coal samples, and the chromatograph quality was fully compliant with the national standard.

1) Equipment materials

(1) Gas Chromatograph GC-4000A

(2) High purity nitrogen: 99.99%

(3) High purity hydrogen: 99.99%

(4) Standard air

(5) Table sample of index gases

2) Instrument operation steps

(1) Instrument start-up and warm-up.

① Hit N<sub>2</sub> , H<sub>2</sub> and Air switch first. Make N<sub>2</sub> pressure: 0.4Mpa~0.5Mpa

Air pressure: 0.3Mpa~0.4Mpa

H<sub>2</sub> Pressure: 0.3Mpa~0.4Mpa

② Ventilate for about 10 minutes and wait for column A (N<sub>2</sub>) column B (N<sub>2</sub>) i.e. column A and B on the chromatograph, with a pressure increase of 0~0.1 MPa.

③ Turn on the chromatograph power switch, open its upper bridge flow button and press Run. (Programming omitted here)

④ Wait until the temperature of column II of the converter has risen to 360°C, then ignite A and B. A poof is heard to indicate successful ignition. You can also use tweezers to put in A, B two columns, by observing the presence of water gas can also be judged, there is then ignited, ignited by the low resistance set to high resistance.

(2) After a period of time, when the baseline is stable, the gas can be analysed.

(3) Inject the gas into the chromatograph through the gas inlet, click on "Acquisition" and after a period of time when all the "peaks" have "gone", click on Stop Acquisition and Save. In the process of analysing the gas sample, the "method" needs to be done first: the difference between the results of two consecutive standard gases is within  $\pm 0.02\%$ , and the results are saved as the "method" for the gas measured in that path, with the 2-way method using the law, and the 3-way method using the external standard. The 3- and 4-way methods use the external standard method. When analysing a gas sample, the method is opened after the sample has been passed, and the amount of gas measured can then be seen through the "preview".

(4) Shutdown

① Close the air.

② Close the bridge temperature switch.

③ Disconnect electrical components and heating power.

④ Keep the carrier gas and hydrogen gas in until the chromatograph has cooled down.

## 4.5.6 Measurement results

The test results are shown in Table 4.1.

**Table 4.1 Experimental gas concentration data for programmed temperature rise**

Temperature/°C	Gas concentration/ppm				
	CO	CO <sub>2</sub>	CH <sub>4</sub>	C <sub>2</sub> H <sub>4</sub>	C <sub>2</sub> H <sub>2</sub>
30	0.28	239.36	15.81	0	0
40	1.74	324.07	19.08	0	0
50	4.61	413.31	20.47	0	0
60	9.91	508.2	22.02	0	0
70	21.62	602.01	27.33	0	0
80	38.30	695.17	33.08	0	0
90	57.33	790.21	35.97	0	0
100	80.66	885.82	39.7	0	0
110	110.85	979.36	46.01	0.21	0
120	170.55	1086.74	53.29	0.30	00
130	259.01	1355.34	63.03	0.36	0
140	396.39	1678.11	74.07	0.98	0
150	597.58	2004.38	82.11	1.24	0
160	890.08	2595.33	91.07	1.52	0
170	1306.31	3759.82	104.37	2.35	0
180	1897.42	5443.11	115.21	3.41	0

In order to make the forecast of natural coal fire timely and accurate, the marker gas chosen for the experiment must have the following conditions.①

(a) Sensitivity: once there is coal in a coal mine shaft in a state of spontaneous combustion and the coal temperature exceeds a certain value, the gas must appear and its generation increases steadily with the increase in coal temperature.② Regularity: there is a good correspondence between the change in concentration of the marker gas and the coal temperature, and the

repeatability is good.③ measurability: the presence of the marker gas can be detected by ordinary chromatographic analysers④ early manifestation: the marker gas must be present at an early stage in the onset of self-heating of the coal to allow for predictive warning.⑤ Uniqueness: a gas that is present only as a result of spontaneous combustion or burning.⑥ Monotonic variability: the concentration rises or falls monotonically with temperature, showing a strong regularity. This chapter therefore uses the single gas indicators CO, CO<sub>2</sub>, C<sub>2</sub> H<sub>4</sub> , C<sub>2</sub> H<sub>2</sub> and the composite indicator CO/CO<sub>2</sub> for the graded prediction of spontaneous combustion of coal in the Tingnan mine.

#### 1). CO generation pattern

Figure 4.4 shows the trend of CO concentration with coal temperature in coal seam No. 4 of Tingnan coal mine. As can be seen from Figure 4.4, CO gas is present at a coal temperature of 30 °C, with a concentration of  $0.28 \times 10^{-6}$ . The production of CO increases slowly until the coal temperature reaches 50-60 °C; when the coal temperature exceeds 50-60 °C, the production of CO increases exponentially; when the coal temperature reaches 100-110 °C, the production of CO increases rapidly and the coal sample enters the stage of intense oxidation reaction. The CO gas production pattern can better reflect the spontaneous combustion characteristics of coal seam No. 4 in the Tingnan coal mine, and can be used as an index gas for the natural ignition of coal seam No. 4 in the Tingnan coal mine.

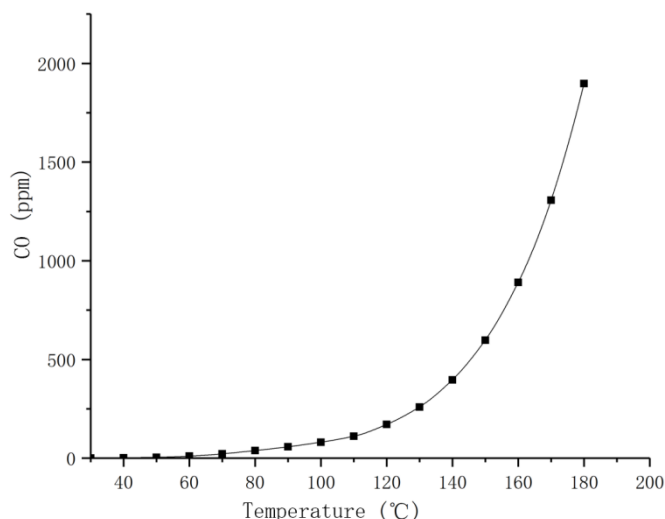


**Fig. 4.4 Trend of CO concentration in coal seam 4 with coal temperature at Tingnan coal mine**

2) CO<sub>2</sub> Production pattern

Figure 4.5 shows the trend of CO<sub>2</sub> concentration with coal temperature in coal seam 4 of Tingnan coal mine. From Figure 4.5, it can be seen that the concentration of CO<sub>2</sub> is 239 x 10<sup>-6</sup> at a coal temperature of 30°C, indicating that the pores of the coal body in this mine contain primary CO<sub>2</sub> gas. The amount of gas produced increases in a largely exponential pattern as the coal temperature increases. As CO<sub>2</sub> is a sorbent gas of the coal in this mine, CO<sub>2</sub> gas is not suitable as an index gas for spontaneous combustion in the No. 4 coal seam of the Tingnan Mine.

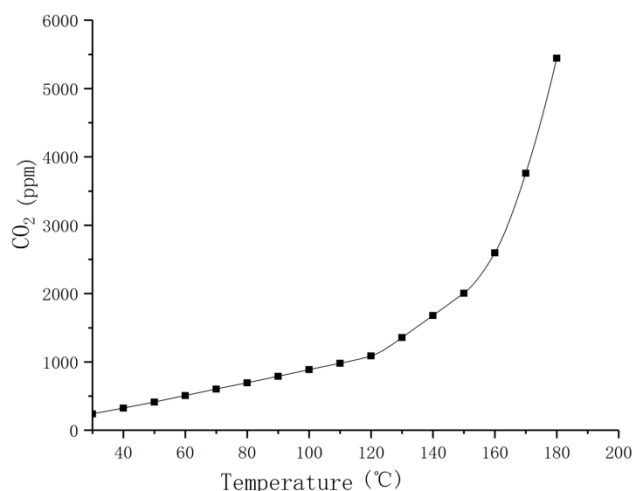


**Fig. 4.5 Trend of CO<sub>2</sub> concentration with coal temperature in coal seam No. 4, Tingnan Coal Mine**

### 3) C<sub>2</sub>H<sub>4</sub> Gas production pattern

The occurrence of C<sub>2</sub>H<sub>4</sub> indicates that the natural firing of the coal has entered the accelerated oxidation stage. Figure 4.6 shows the trend of C<sub>2</sub>H<sub>4</sub> concentration with coal temperature in coal seam No. 4 of Tingnan coal mine. From Figure 4.6, C<sub>2</sub>H<sub>4</sub> gas appears at 110 °C with a concentration of  $0.21 \times 10^{-6}$ , and its production quantity increases exponentially with the increase of coal temperature, and increases rapidly after 160°C, and the concentration of C<sub>2</sub>H<sub>4</sub> gas is  $3.41 \times 10^{-6}$  at 180°C. C<sub>2</sub>H<sub>4</sub> gas production quantity varies well with coal temperature, therefore, C<sub>2</sub>H<sub>4</sub> gas can be used as the index gas of natural ignition in coal seam

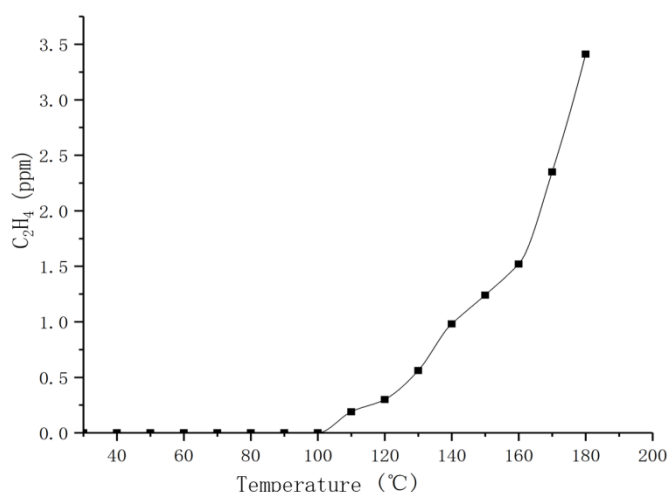


**Fig. 4.6 Trend of C<sub>2</sub>H<sub>4</sub> concentration with coal temperature in coal seam 4 of Tingnan coal mine**

### 4) C<sub>2</sub>H<sub>2</sub> Generating laws

C<sub>2</sub>H<sub>2</sub> arises only during the violent oxidation phase of the coal and has a strong temperature interval characteristic. Although C<sub>2</sub>H<sub>2</sub> did not occur under the experimental conditions from 30 to 200°C, once C<sub>2</sub>H<sub>2</sub> was detected downhole, it indicated that the coal temperature had exceeded 200°C, indicating that the coal had undergone a violent chemical reaction. Therefore, it is recommended that C<sub>2</sub>H<sub>2</sub> be used as one of the index gases for the intense oxidation stage of coal seam 4 in the Tingnan coal mine.

### 5) Ratio of CO to CO<sub>2</sub>

CO is a relatively sensitive marker gas during the natural firing of coal. Due to the complex downhole conditions, the location where CO is detected is not necessarily a high temperature point, and CO is diluted by the large amount of seeping air and its concentration varies with the wind flow. Therefore, it is difficult to determine the actual spontaneous combustion condition of a loose coal body from CO concentration alone. Using the CO/CO<sub>2</sub> ratio to determine the condition of spontaneous coal combustion eliminates the effect of wind flow size on gas concentration.

Figure 4.7 shows the trend of CO/CO<sub>2</sub> ratio with coal temperature in coal seam No. 4 of Tingnan coal mine. In the low temperature oxidation stage, the CO/CO<sub>2</sub> ratio is small, and at 60°C, the CO/CO<sub>2</sub> ratio is 0.05; in the accelerated oxidation stage, the CO/CO<sub>2</sub> ratio starts to increase, and at 110°C the ratio is 0.26 and at 200°C the ratio is 0.43. The CO/CO<sub>2</sub> ratio curve has a good regularity, therefore, the CO/CO<sub>2</sub> ratio is recommended as a composite indicator for the natural ignition of coal seam No. 4 in the Tingnan coal mine. The composite index of the preferred marker gas.

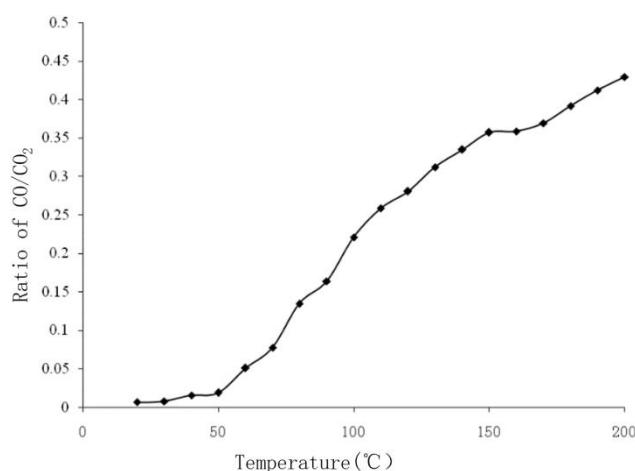


**Fig. 4.7 Trend of CO/CO<sub>2</sub> ratio with coal temperature in coal seam 4 of Tingnan coal mine**

#### 6) Characteristic temperature of spontaneous combustion of coal

By analysing the gas generation patterns and ratios of the natural fire index gas preferences test for the No. 4 coal seam at Tingnan Coal Mine, the characteristic temperature range for spontaneous combustion can be derived.

Table 4.2 shows the characteristic temperature range and gas characterisation of the preferred natural fire index gas test for the No. 4 coal seam in the Tingnan Mine.

**Table 4.2 Characteristic temperatures and their gas characterisation for the preferred natural fire signalling gas test in the No.4 coal seam at Tingnan Mine**

Characteristic temperature Name	Preferred gas selection experiment for natural fire indicator in No.4 coal seam at Tingnan Coal Mine		Remarks
	Characterisation parameters	Temperature/°C	
Critical temperature	Increased decrease in oxygen concentration. The rate of warming increases slowly.	50 to 60	Small molecules in coal that oxidise easily, bonds that break easily and a few functional groups that react easily
Dry cracking temperature	Producing gases such as ethane and ethylene. Release of large amounts of volatile fractions.	100 to 110	Large changes in the molecular structure of coal, resulting in free radicals, accelerated breakage and cleavage of side chains, bridge bonds, etc.



---

## 5 Conclusion

---

(1) Through the thermogravimetric experiments of the coal samples from Tingnan, the effects of oxygen concentration, heating rate and particle size on the TG, DTG and DSC curves during the thermal decomposition of the coal were analysed, and the relationship between the characteristic temperature points of the coal and the reaction kinetic parameters was also analysed. At the same time, by analysing the characteristic gases of thermal decomposition of coal and the functional groups of coal, the structure of functional groups within the coal of Tingnan was analysed to provide a theoretical basis for the study of coal spontaneous combustion, and the following conclusions were drawn: ① With the increase of oxygen concentration, the curve of thermal decomposition of coal shifted towards the low temperature. ② With the increase of the heating rate, the TG and DSC curves of coal show hysteresis, while the DTG curve shifts forward and the rate increases. (iii) As the particle size decreases, the TG, DTG and DSC curves all move forward. The maximum weight loss rate value of the coal becomes larger, the temperature value at which the ignition point is reached decreases, and the reaction range for oxidative ignition of the coal is shortened, i.e. the total time for oxidative spontaneous combustion of the coal is shortened. ④ The activation energy of the coal samples were ranked as follows:  $E_{\text{Xingtao}} < E_{\text{Tingnan}} < E_{\text{Xing County}} < E_{\text{Tangshan}}$ , according to which the lower the activation energy, the more likely the coal is to spontaneously ignite and therefore the Tingnan coal mine is prone to ignition.

(2) By means of theoretical derivation, the effects of fresh air flow dilution, nitrogen injection and gas gushing on CO and its indicators in the mined area were studied, and it was concluded that the carbon oxide ratio was the only indicator that was not affected by fresh air flow, nitrogen injection and gas gushing, so the carbon oxide ratio was selected as an indicator for coal spontaneous combustion warning.

(3) The natural ignition index gas index of coal samples from the Tingnan coal mine was measured by the natural ignition index gas preference experimental system. The following conclusions were obtained ① The critical temperature of natural ignition of coal No. 4 from Tingnan coal mine was 50-60°C, representing the stage

of self-heating acceleration and negative combustion of coal; the dry cracking temperature was 100 - 110°C, representing the stage of self-ignition of coal about to enter fire. ②The main indicators of natural ignition of coal No.4 in Tingnan coal mine are CO, C<sub>2</sub>H<sub>4</sub> and C<sub>2</sub>H<sub>2</sub>. CO concentration  $\geq 55.41 \times 10^{-6}$  was detected and there is an obvious increasing trend, indicating that natural ignition has occurred; C<sub>2</sub>H<sub>4</sub> concentration  $\geq 1 \times 10^{-6}$  was detected, representing coal seam temperature  $\geq 130^\circ\text{C}$ ; C<sub>2</sub>H<sub>2</sub> gas concentration  $\geq 1 \times 10^{-6}$  was detected, representing coal seam temperature  $\geq 200^\circ\text{C}$ . ③The auxiliary index of natural ignition of coal No.4 in Tingnan coal mine is CO/CO<sub>2</sub>.

---

## Reference

---

Zeng, F. P, H. Zhang, and F. R. Zeng . "Mine fire prevention and control along goaf side of fully mechanized longwall top coal caving mining face." *Coal Science and Technology* (2006).

Xu J and Chen X. "Research progress on mechanism and prediction theory of coal spontaneous combustion." *Journal of Liaoning University of Technology : Natural Science Edition* (2003).

Wang, H., B. Z. Dlugogorski , and E. M. Kennedy. "Theoretical analysis of reaction regimes in low-temperature oxidation of coal." *Fuel* (1999).

Lu G., Geng M. "Research status of coal spontaneous combustion mechanism and prevention technology in goaf." *Journal of Liaoning University of Technology : Natural Science Edition* ( 2009 ).

Chen C, Qi Q. "Development status and trend of mine fire prevention technology." *Coal technology* (2009).

Wang S, Zhang G. "Mine fire prevention." *China University of Mining and Technology Press* (1990).

Lu Wei. "Rapid identification method of coal spontaneous combustion tendency based on oxygen consumption." *Journal of Hunan University of Science and Technology* (2008).

Liang Y, Luo H. "Current status and trend of coal mine fire prevention technology in China." *Journal of China Coal Society* (2008).

Luo H, Qian G. "Research on index gas indicators of spontaneous combustion of various coal types." *Coal Mine Safety* (2003).

Zhang X, Xi G, Chen X. "Division of spontaneous combustion hazard areas and prediction of spontaneous combustion in short-distance coal seam mining." *Journal of China Coal Society* (2005).

Cui Hi, Wang Z, Wang H. "Early prediction technology of coal seam spontaneous combustion and its application." *Coal Mine Safety* (2001).

---

Yang H, Luo H. "Experimental study on the identification of coal mine fires with bionic odor sensor array." *Journal of China Coal Society* (2007).

Deng J, Xu J, Chen X. "Research progress on coal spontaneous combustion mechanism and prediction theory" *Journal of Liaoning Technical University* (2003).

Wang D, Xin H, Qi X, Dou G. "Various elementary reactions and their relationships in coal spontaneous combustion: coal oxidation kinetics theory and application. " *Journal of China Coal Society* (2014)

You F, Huang F, Wen H. "Analysis of coal heating oxidation and coal oxygen complex characteristics based on thermogravimetric analysis. " *Journal of Safety and Environment* (2018).

Yang Yi. "Research on mechanism and performance of coal spontaneous combustion inhibitor based on oxidation characteristics. " *Xi'an University of Science and Technology* (2015).

Fei Jinbiao. "Research on the theory of coal spontaneous combustion stage and the classification early warning method." *Xi'an University of Science and Technology* (2019).

Badzioch, S., and P. Hawksley . "Kinetics of Thermal Decomposition of Pulverized Coal Particles." *Industrial & Engineering Chemistry Process Design and Development* 9.4(1970).

Frazier G C , Mason C , D Stickle, et al. "Effectiveness of SO<sub>2</sub> sorbents by thermogravimetry-combustion with coal". *Fuel*, (1982).

Solomon P R , Carangelo R M . FT-IR analysis of coal. (1988).

Dong K, Sang S, Yong T et al. "Study of coal pyrolysis by thermo-gravimetric analysis (TGA) and concentration measurements of the evolved species." *Journal of Analytical and Applied Pyrolysis* (2011).

Landry, M. R. "Thermoporometry by differential scanning calorimetry: experimental considerations and applications." *Thermochimica Acta* (2005)

Qiao, et al. "Investigation on the effect of particle size and heating rate on pyrolysis characteristics of a bituminous coal by TG-FTIR." *Journal of Analytical & Applied Pyrolysis* (2016)

---

Zhang Yanni et al. "TG/DTG experiment of Huating coal spontaneous combustion characteristic temperature." Journal of Xi'an University of Science and Technology (2011)

Wu Jinguang. "Modern Fourier Transform Infrared Spectroscopy Technology and Application". Science and Technology Literature Publishing House (1994)

Xue Ning, Yao Wei. "Determination of kinetic parameters of coal combustion reaction." Thermal Power Generation (2011)

Xie Huaqing, Yu Qingbo, Li Peng. "Description of kinetic characteristics of coal gasification reaction and solution of kinetic parameters." Proceedings of the 2010 National Annual Conference on Energy and Thermal Engineering (2010)

Ju Yiwen et al. "Fourier Transform Infrared Spectroscopy Study on the Stress Effect of Tectonic Coal Structural Components." Spectroscopy and Spectral Analysis (2005)

Kou Liwen et al. "Analysis on the production law and influencing factors of spontaneous combustion index gas in Wenzhuang coal." Coal Mine Safety (2012)

Yu Jian. "Research on the influence of coal sample quality on the regularity of coal spontaneous combustion index gas generation." Mining Safety and Environmental Protection (2014)

Luo Dayong, Liu Zhen. "Optimization and Application of Coal Spontaneous Combustion Index gas in Xutuan Coal Mine." Mining Safety and Environmental Protection (2021)

Xia Hua et al. "A real-time online remote monitoring device and method for multi-component coal spontaneous combustion index gas." (2016)

Wang Zhenping. "Basic Research on Determination Technology of Coal Spontaneous Combustion Based on Index gas. Diss". Xi'an University of Science and Technology (2006)



中国矿业大学(北京)  
CHINA UNIVERSITY OF MINING & TECHNOLOGY-BEIJING

### Thesis Grade

Thesis Topic: Study on the Mechanism of Spontaneous Combustion  
of Coal and Its Index Gases in Tingnan Coal Mine

Author: Yuyi Xie

Supervisor: Hongqing Zhu Grade: 88

Signature: 朱红青

Co-supervisor: \_\_\_\_\_ Grade: \_\_\_\_\_ Signature: \_\_\_\_\_